Title: Genetic Foundations of Neurophysiological and Behavioural Variability Across the Lifespan.

Authors: Jason da Silva Castanheira[1], Jonathan Poli[1,2], Justine Y. Hansen[1], Bratislav Misic[1], Sylvain Baillet[1, †]

Affiliations:
[1] Montreal Neurological Institute, McGill University, Montreal QC, Canada
[2] CentraleSupélec, Université Paris-Saclay, Paris, France

[†] Corresponding author: sylvain.baillet@mcgill.ca

Abstract: Neurophysiological brain activity underpins cognitive functions and behavioural traits. Here, we sought to establish to what extent individual neurophysiological traits spontaneously expressed in ongoing brain activity are primarily driven by genetic variation. We also investigated whether changes in such neurophysiological features observed across the lifespan are supported by longitudinal changes in cortical gene expression. We studied the heritability of neurophysiological traits from task-free brain activity of monozygotic and dizygotic twins as well as non-related individuals recorded with magnetoencephalography. We found that these traits were more similar between monozygotic twins compared to dizygotic twins, and that these heritable core dynamical properties of brain activity are predominantly influenced by genes involved in neurotransmission processes. These genes are expressed in the cortex along a topographical gradient aligned with the distribution of major cognitive functions and psychological processes. Our data also show that the impact of these genetic determinants on cognitive and psychological traits increases with age. These findings collectively highlight the persistent genetic influence across the lifespan on neurophysiological brain activity that supports individual cognitive and behavioural traits.

Lay summary

Our study investigates how patterns of brain activity that shape our thinking and behaviour might be inherited. We compared the brain-activity profiles of identical twins, fraternal twins, and unrelated individuals and discovered a closer match between those of identical twins, compared to fraternal twins and unrelated individuals. This suggests that brain-activity profiles, akin to other biological attributes, are largely inherited. We identified a set of genes most strongly associated with individual brain-activity profiles. These genes are known to shape how brain cells communicate, along with other essential neurobiological functions, particularly in brain areas crucial for cognition and attention. The influence of these genes evolves and grows as we age. In summary, our study advances the understanding that our individual brain-activity profiles, much like our physical attributes, are significantly shaped by genetics throughout our lives, influencing the person we become.

Keywords

Neurophysiology, Heritability, Genetic determinants, Brain-fingerprints, Magnetoencephalography (MEG), Monozygotic and dizygotic twins, Ion transport, Neurotransmission, Neurodevelopment, Cognitive and affective brain functions.

Graphical abstract

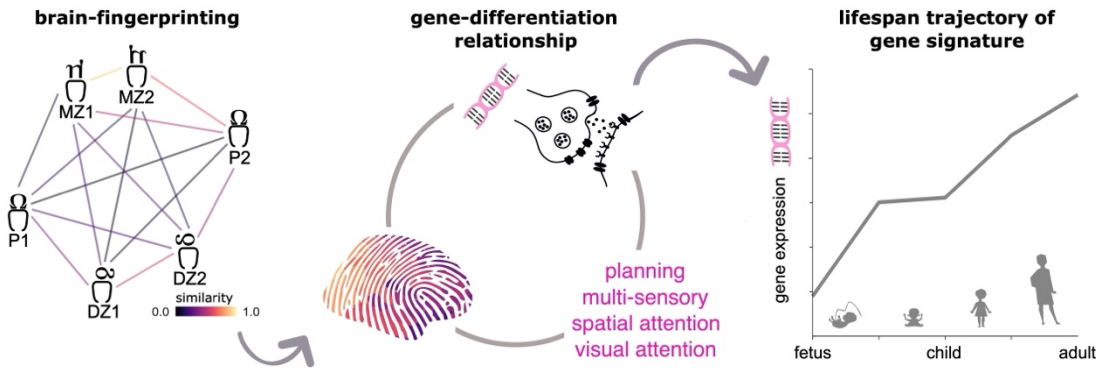

This study examines the relationship between individual patterns of neurophysiological brain activity and gene expression profiles. First, the researchers successfully differentiated individuals based on their brain activity at rest by comparing the similarity of 'snapshots' of brain activity at different time points. If the brain activity of a participant is most similar to themselves across two recordings, that participant is said to be correctly differentiated. The study reports that the brain-fingerprints of monozygotic (MZ) twins are remarkably similar between siblings, unlike those of dizygotic (DZ) twins. Second, the study identified specific gene expression patterns associated with distinctive neurophysiological traits and major cognitive functions such as planning, multi-sensory processing, spatial attention, and visual attention. Third, the prominence of these gene expression patterns increases with neurodevelopment, suggesting that genetic factors contribute to the evolution of cognitive functions over the lifespan, from fetal stages through adulthood.

Main Text:

Several recent neuroimaging studies have shown that ongoing brain activity at rest, without performing a specific task, defines a neurophysiological profile unique to each person. Unlike hand fingerprints, these *brain-fingerprints* are associated with individual cognitive traits and are altered by pathology (*1–9*), forming a distinct personal neurophysiological profile. Whether a person's genotype is associated with their neurophysiological profile is currently unknown. Heritability studies of inter-individual variability (*10*) have reported some genetic associations with brain structures (*11–14*) and activity (*15–20*). Genetic factors determine, to some extent, inter-individual variations in broad cognitive domains such as attentional and general intellectual abilities (*21–25*). Here, we studied how both individual neurophysiological and cognitive profiles relate to the expression of specific genes across the lifespan.

We used task-free magnetoencephalographic (MEG) imaging (*26*) to derive the individual neurophysiological profiles (*2*) of monozygotic (MZ) and dizygotic (DZ) twins, along with unrelated individuals. We hypothesized that if neurophysiological brain activity is determined by genetic factors, then the neurophysiological profiles of MZ twins, who share nearly identical genomes, would be nearly identical, unlike those of DZ twins (*27*). We then identified which genes are related to the features that differentiate individuals based on their neurophysiological profiles. Additionally, we investigated whether the genetic influence on these neurophysiological traits is linked to major psychological processes that characterize individual traits and how this influence evolves across the lifespan.

Results:

Individual Neurophysiological Profiling and Differentiation

We derived the neurophysiological profile of 89 individuals (17 pairs of monozygotic twins, 11 pairs of dizygotic twins, and 33 unrelated individuals; 22-35 years old) from three 6-minute task-free MEG recordings provided by the Human Connectome Project(*28*). We derived individual profiles from the distribution of neurophysiological signal power of MEG activity across the cortex for each recording (*2*) (see Methods).

We first assessed the accuracy of inter-individual differentiation based on the neurophysiological profiles obtained from the three recordings of each participant (Figure 1A). The accuracy of inter-individual differentiation from these neurophysiological profiles was 83.4% (95% bootstrapped CI [73.8, 90.0]) across a broad frequency spectrum of brain activity ([1-150 Hz]). The high temporal resolution of the data enabled to study how the accuracy of neurophysiological profiling varied between the prototypical frequency bands of electrophysiology. Inter-individual differentiation varied substantially across these frequency ranges, from 59.7% in the delta band (1-4 Hz; [57.5, 73.8]) to 87.4% in the high-gamma band (50-150 Hz; [80.0, 92.5]) as detailed Figure 1B.

We then evaluated the similarity between the neurophysiological profiles of siblings in a twin pair (Figure 1A), finding that those of monozygotic twins matched with 61.5% accuracy ([46.7, 76.7]).

In contrast, the profiles of dizygotic twins showed a considerably lower match accuracy of only 5.2% ([0.0, 15.0]; Figure 1B). These differences in matching accuracies between monozygotic and dizygotic twins varied across the frequency bands of neurophysiological brain activity as shown in Figure 1B. The discrepancies were particularly pronounced in the alpha band (8-13 Hz), where MZ twins matched with an accuracy of 47.8% ([33.3, 66.7]) compared to only 1.2% for DZ twins ([0.0, 5.0]). In the beta band (13-30 Hz), accuracies were 52.1% for MZ twins ([33.3, 70.0]) versus 7.1% for DZ twins ([0.0, 20.0]).

Heritability of Neurophysiological Traits

Leveraging intra-class correlation (ICC) statistics(*2*, *3*, *29*) (see Methods), we found that cortical activity in the theta (4-8 Hz; average ICC = 0.74), alpha (8-13 Hz; ICC = 0.83), and beta (13-30 Hz; ICC = 0.74) frequency bands are the most distinctive traits of neurophysiological profiles between individuals (Figure 1C). These traits are heritable, with Falconer's method showing a mean heritability (H^2) of 0.85 for theta-band traits, 0.76 for alpha-band traits, and 0.77 for beta-band traits across the temporal, frontal, and occipital cortex (Figure S4A). The neurophysiological traits of the occipital visual regions(*30*) were the most heritable, while those of the limbic network were the least heritable (Figure S4A, right).

Although we reported above that the neurophysiological profiles of MZ twins match each other more closely than those of the general population, the neurophysiological profile of each MZ twin remains distinguishable from their sibling. This might suggest that individual-specific features stand apart from the heritable aspects of their neurophysiological profile. However, our results show that the most differentiable features of neurophysiological profiles tend to be heritable. To test this, we measured the spatial alignment between the ICC maps of the most salient individual features of neurophysiological profiles (Figure 1C) and the heritability maps (Figure S4A). We found positive spatial correlations across broadband cortical signals (1-150 Hz; $r = 0.28$, $p_{spin} = 0.026$), and specifically in the alpha ($r = 0.62$, $p_{spin} = 0.0009$) and beta ($r = 0.58$, $p_{spin} = 0.0009$) bands (Figure S4B). These findings confirm that the most distinctive features of neurophysiological profiles tend to be heritable, further emphasizing the genetic basis for the neurophysiological characteristics that distinguish individuals.

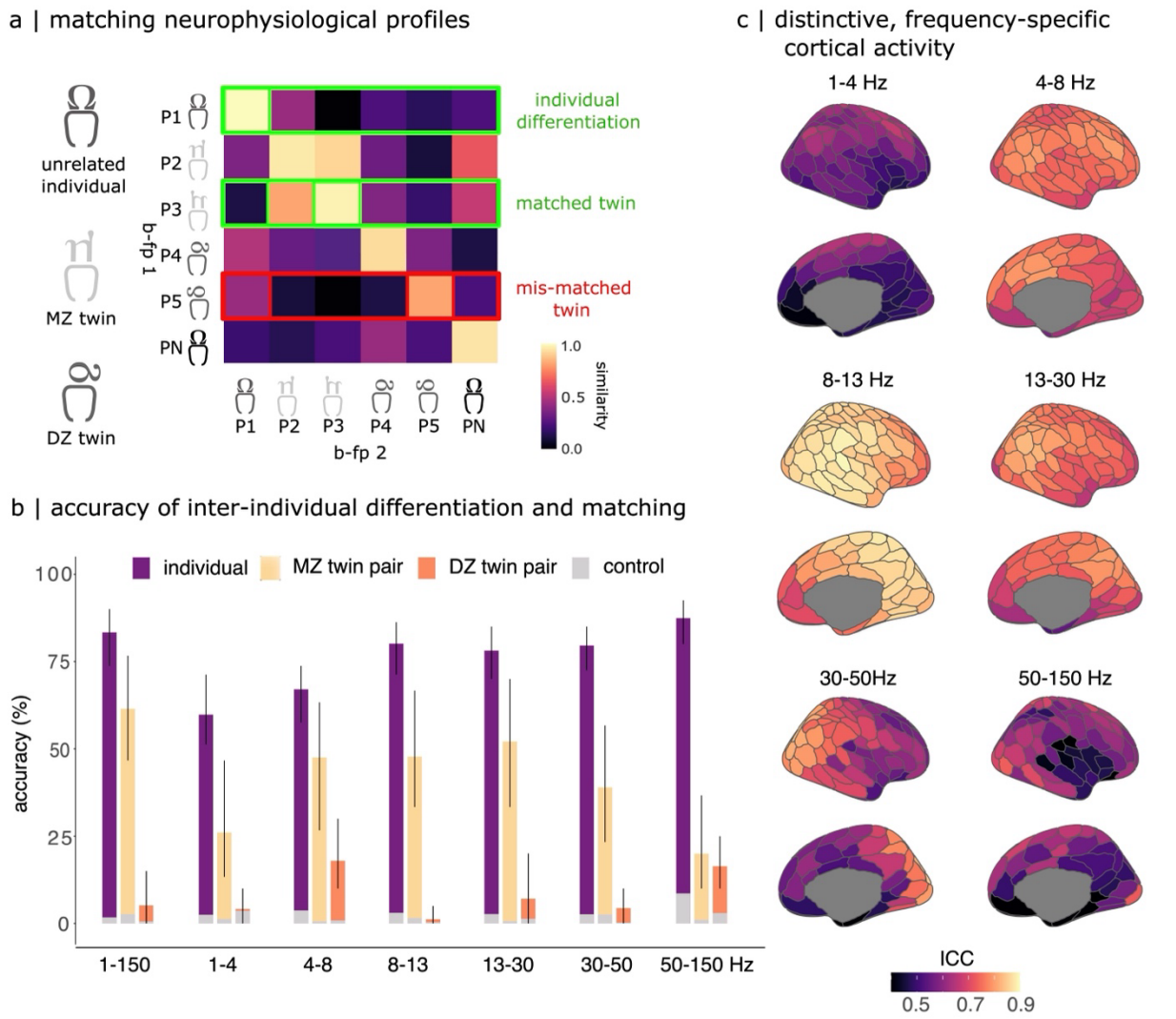

Fig. 1. Neurophysiological Profiling.

(a) The color-coded array reports the similarity between the neurophysiological profiles within (self-similarity; diagonal elements) and between (similarity with others; off-diagonal elements) individuals. The similarity is measured using cross-correlation coefficients derived between the neurophysiological profiles of each individual across all three datasets. A participant is correctly differentiated based on their brain-fingerprint if their neurophysiological profile remains similar across the three datasets. Using these statistics, we also assessed how well the neurophysiological profile of a twin matched their sibling's profile compared to any other individual in the cohort.

(b) The purple bar graphs report the inter-individual differentiation accuracy between all individuals in the cohort. The bar graphs in shades of orange indicate the matching accuracy between twin pairs. The data are reported with 95% confidence intervals for broadband (1-150 Hz) and specific frequency bands of neurophysiological brain activity: delta (1-4 Hz), theta (4-8 Hz), alpha (8-13 Hz), beta (13-30 Hz), gamma (30-50 Hz), and high gamma (50-150 Hz). Control

statistics are presented to rule out the possibility that environmental conditions around each participant's recording biased the accuracy of inter-individual differentiation (grey bar graphs). (c) Topographic maps highlight the regions with the most salient neurophysiological activity per frequency band that differentiate between individuals, as measured with intra-class correlation (ICC) statistics (see Main Text and Methods).

Neurophysiological Profiles are Aligned with Cortical Gene Expression

We then assessed whether the most salient individual traits of the neurophysiological profiles (ICC maps of Figure 1C) also align topographically with genetic cortical expressions. To do this, we studied the spatial covariation of the ICC of neurophysiological profiles with maps of cortical gene expressions with greater differential stability (>0.1) (*31–35*), retrieved from the microarray Allen Human Brain Atlas (*33*), using Partial Least Squares (PLS) correlation. We found a single PLS component significantly accounting for 85.2% of the covariance (CI [73.4, 90.1], $p_{spin} = 0.01$; Figure S5A). This analysis revealed a topographical pattern where visual and somatomotor regions exhibited positive covariance with genetic expressions, while limbic regions exhibited negative covariance (Figure S5B). This indicates that the most differentiable traits of individual neurophysiological profiles are spatially aligned with specific gene expression patterns along the cortical surface. We cross-validated this observation with 1,000 permutations corrected for spatial autocorrelation, resulting in a median out-of-sample correlation of r = 0.64 ($p_{spin} = 0.002$; Figure S5C).

We then measured how each frequency range of cortical activity contributed to this alignment between cortical gene expression and the salient traits of neurophysiological profiles. We found that all frequency ranges contributed exclusively positively to this association: delta (r = 0.52, 95% CI [0.45, 0.61]), alpha (r = 0.63, 95% CI [0.58, 0.69]), beta (r = 0.52, 95% CI [0.42, 0.62]), gamma (r = 0.71, 95% CI [0.66, 0.76]), and high gamma bands (r = 0.43, 95% CI [0.34, 0.53]; Figure 2A) with the exception of the theta band (r = 0.07, 95% CI [-0.09, 0.22]).

Genes and Cell Types Associated with Neurophysiological Traits

We then investigated which genes' expressions contribute the most to the reported association with neurophysiological traits, aiming to identify the biological functions associated with these genes and the specific cell types involved. We selected the top 2,208 genes based on their highest positive loadings in the PLS analysis and the top 2,344 genes based on their highest negative loadings. We performed a gene ontology (GO) analysis using the ShinyGO pipeline and resources from the GO database (*36*), which revealed distinct biological processes linked to these sets of genes (see Methods). Genes with positive loadings were enriched in biological processes such as ion transport, synaptic functioning, and neurotransmitter release, while genes with negative loadings were associated with processes like development, neurogenesis, and cell morphogenesis (Figure 2B, right panel; complete gene list in Supplemental Information).

To determine the types of cells corresponding to these genes, we analyzed gene sets that are preferentially expressed in seven cell types as determined by RNA sequencing studies(*37–42*). We found an overrepresentation of genes with positive loadings in excitatory neurons (p_{FDR}= 0.002; 1,000 gene permutations, two-tailed, FDR: corrected for false discovery rate) and inhibitory neurons (p_{FDR} = 0.006). Conversely, genes with positive loadings were underrepresented in astrocytes (p_{FDR} = 0.002) and oligodendrocyte precursor cells (OPCs; p_{FDR} = 0.03). Genes with negative loadings were predominantly represented in astrocytes (p_{FDR} = 0.002), microglia (p_{FDR} = 0.004), and oligodendrocytes (p_{FDR} = 0.002), but were less represented in OPCs (p_{FDR} = 0.002; Figure 2B left panel).

These findings suggest a clear dichotomy: genes that show positive loadings and thus positively correlate with the distinctive traits of neurophysiological profiles are predominantly expressed in neurons, whereas genes with negative loadings, indicating a negative correlation with these traits, are more frequently expressed in neuron-supporting cells such as astrocytes and microglia. Our results are consistent with existing models of the physiological origins of MEG signals (*26*, *43*, *44*).

Association with Neuropsychological Processes

Building on prior work reporting associations between brain-fingerprint features and cognitive traits (*1–3*, *45*, *46*) as well as genetic influences on inter-individual variations in cognitive domains (*21–25*), we investigated how the gene-neurophysiological associations discovered in our data may relate to neuropsychological processes.

To investigate this, we performed another PLS analysis to determine how cortical gene expression align topographically with typical cortical maps of neuroimaging activations associated with a range of psychological processes. A single significant component accounted for 67.2% of this covariance (CI [54.7, 72.2%], p_{spin} = 0.002), highlighting a distinction between cognitive and emotional domains (Figure 2C): negative loadings were associated with processes related to emotions, mood, and arousal, whereas positive loadings were linked to attentional, planning, and multimodal sensory processes.

We found that these patterns of covariance between gene expression and psychological processes were strongly aligned with those linking gene expression to individual neurophysiological traits (r=0.99, $p_{spin} < 0.001$; Figure S6, middle and right panels; see also Supplemental Information).

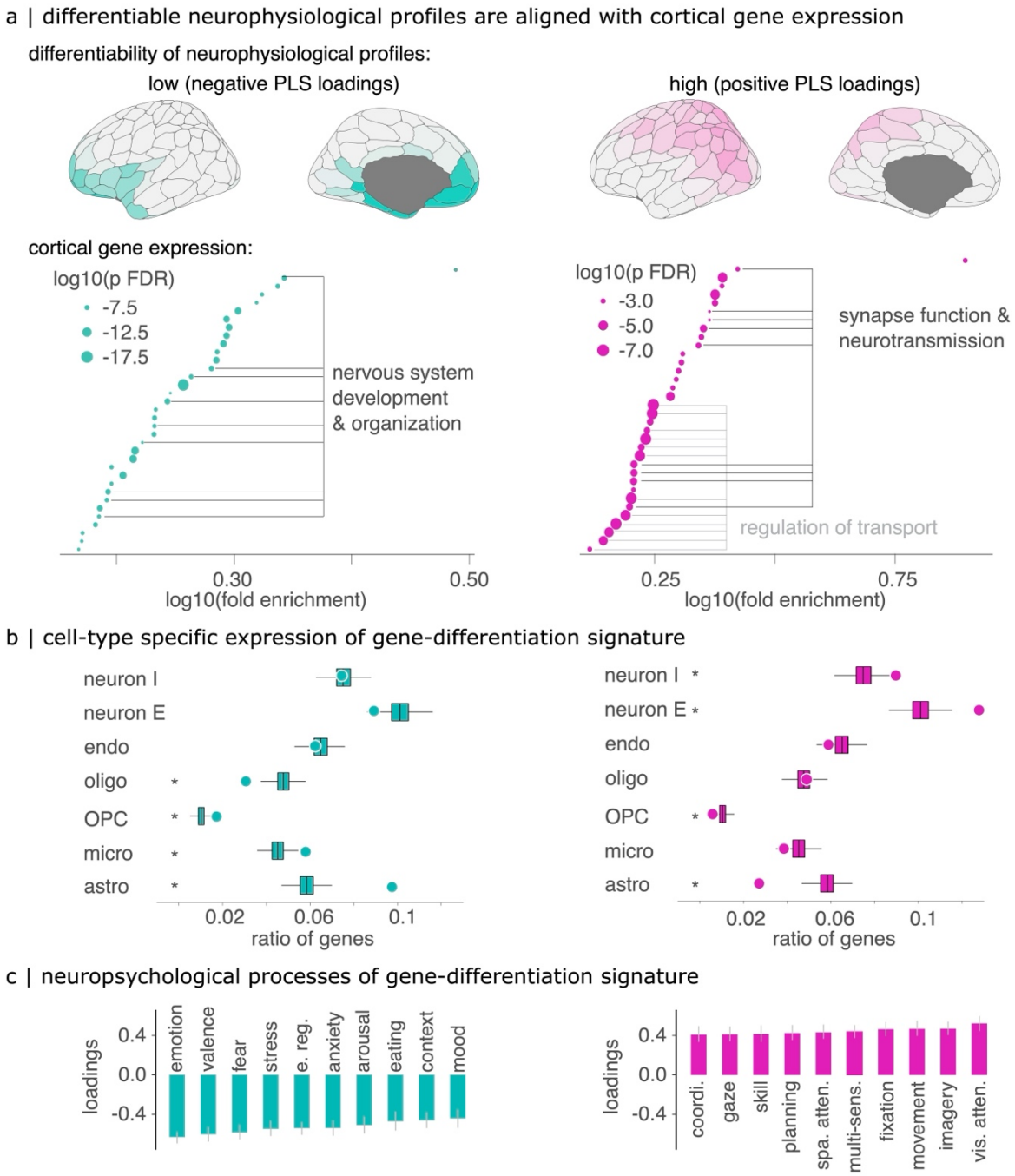

Fig. 2. Associations Between Neurophysiological Traits, Cortical Gene Expression and Neuropsychological Processes.

(a) Contribution of differentiable neurophysiological traits and specific genes to the gene-differentiation signature identified in the PLS analysis. The top panel shows neurophysiological brain score patterns for positive and negative loadings, indicating which cortical parcels align with the observed covariance pattern. All frequency bands, except for theta, contribute significantly to the neurophysiological brain score.

The bottom panel highlights the results of the biological processes gene ontology analysis for both positive and negative loadings. Each point represents a different biological process that is

enriched in the positive and negative gene sets. The size of each point indicates the p-value associated with each biological process. For visualization purposes, we grouped related terms together using horizontal bars.

(b) Cell-type deconvolution analyses, revealing the ratio of genes (both positive and negative) preferentially expressed in seven distinct cell types as identified in prior single-cell and single-nucleus RNA sequencing studies(*37–41*, *47*). The significance of these ratios was evaluated using permutation tests (*p < 0.05). Points represent observed ratios, and box plots depict the distribution of ratios obtained from permuting gene sets. Key: 'neuron I' refers to inhibitory neurons, 'neuron E' to excitatory neurons, 'endo' to endothelial cells, 'oligo' to oligodendrocytes, 'OPC' to oligodendrocyte precursor cells, 'micro' to microglia, and 'astro' to astrocytes.

(c) Analysis of the Gene-Neuropsychological Processes PLS Latent Component: This panel illustrates the top 10 psychological terms that most significantly contribute negatively (cyan) and positively (pink) to the latent component identified in the gene-neuropsychological processes PLS analysis. The cortical maps show the brain score pattern for these neuropsychological terms with both positive and negative loadings. The bar graphs feature the loadings of neuropsychological terms, with pink for positive and cyan for negative terms. Confidence intervals were computed via bootstrapping and therefore are not necessarily symmetric. Terms in the top quartile of loadings delineate a cognitive-affective gradient, with positive loadings on cognitive processes like visual attention and negative loadings on affective processes such as emotion regulation.

Developmental Trajectory of the Gene-Differentiation Signature

Previous work has established that genetic influences on neuropsychological processes become more pronounced with development (*23*, *25*, *48*). Following our identification of the cortical topography of a gene-differentiation signature that aligns with brain activations associated with neuropsychological processes, we tested whether the strength of this gene-differentiation signature also increases throughout development. To test this hypothesis, we assessed the topographical alignment between the cortical expression of genes across life stages in 12 cortical regions (*49*) and that of the gene-differentiation signature. We found that this alignment (i.e., slope) was stronger in later life stages in all tested cortical regions, except for the hippocampus (Figure 3). These findings suggest that the association between gene expression patterns and individual neurophysiological profiles becomes more pronounced throughout development.

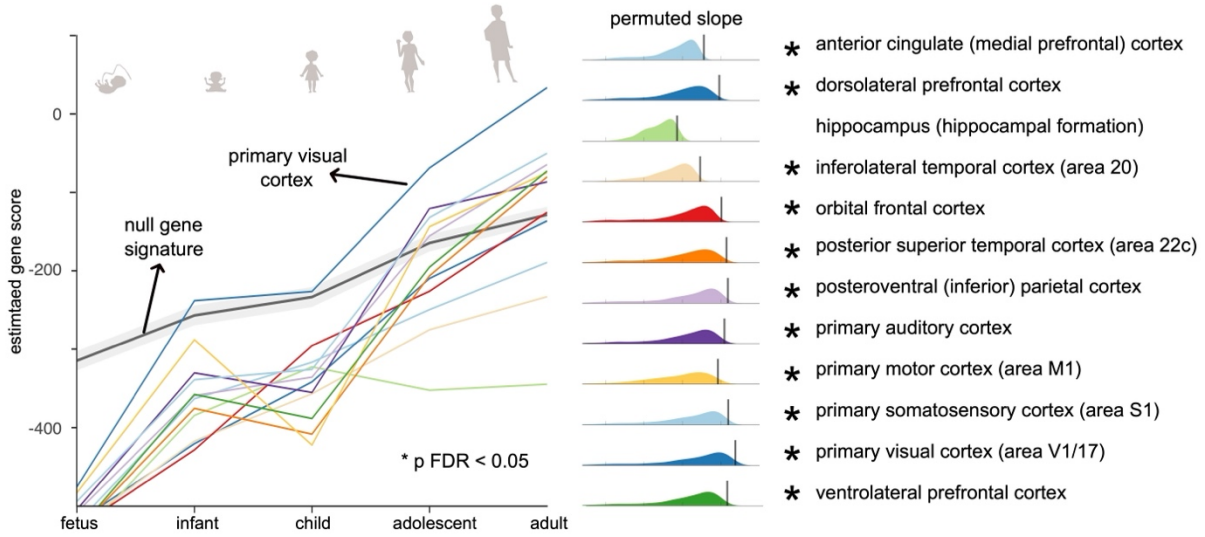

Fig. 3. Strengthening of the Gene-Differentiation Signature Across the Lifespan.

The left panel illustrates the increasing prominence of gene scores through maturation across 12 brain regions based on the BrainSpan data(*49*). The line with the grey shaded area indicates the trajectory of gene scores derived from random auto-correlation preserving permutations of the gene expression data. The right panel presents histograms of permuted slopes for each cortical region. A vertical tick mark shows the observed slope of gene score development, with asterisks denoting significant strengthening of the gene-differentiation signature across development (*$p_{FDR} < 0.05$).

Discussion:

Patterns of brain activity can differentiate between individuals, akin to hand fingerprints (*1–3*, *50*). However, these brain-fingerprints are associated with neuropsychological traits (*1*, *2*, *45*, *46*) and pathophysiology (*6*, *7*, *29*). We investigated the genetic bases of individual neurophysiological profiles.

Heritability of Neurophysiological Traits

Our data show that some of the neurophysiological traits that shape individual profiles are heritable. The neurophysiological profiles of monozygotic twin pairs match each other beyond what can be explainable by mere neuroanatomical resemblances (Figure 1B & Figure S2). Conversely, the differences between the neurophysiological profiles of dizygotic twins are as significant as those between unrelated individuals. These observations underscore that neurophysiological traits are in part shaped by genetics.

The neurophysiological traits of alpha and beta-band activity in parietal cortical regions showed particularly strong heritability (Figure S4), confirming previous observations of the heritability of the individual frequency of alpha activity in humans (*15*, *16*). We observed a connection between these brain rhythms and brain transcriptome gradients. These gradients correlate with brain activations during cognitive tasks, suggesting a deeper genetic-based influence on neurophysiological variability.

A Gene-Differentiation Signature

Gene expression profoundly impacts brain structures and functions (*32*, *47*, *51–55*), such as cortical folding and connectivity within brain networks (*12*, *56*, *57*). Our study extends these findings by demonstrating that, in addition to anatomical and brain-network properties, genetics also shape task-free, ongoing neurophysiological brain activity. This activity reflects a set of distinctive neurophysiological traits, uniquely defining an individual's profile in relation to the cortical expression of specific genes, forming a gene-differentiation signature.

Using gene expression atlases, we found that these traits are related to the expression of genes regulating ion transport and neurotransmission. Genetic variants and variations in gene expression levels likely influence the function of these genes, contributing to the observed inter-individual differences in neurophysiological profiles. Notable genes previously reported as major elements of neurochemical signalling include the catechol-O-methyltransferase (COMT) enzyme, crucial for dopamine metabolism(*58*); the adenosine A2A receptor gene (*59*); adenosine deaminase gene; regulators of glutamatergic receptor channels (*16*); and the GABAB receptor (GABABR1) (*60*), which are. This aligns with previous research that identified related genetic variants modulating alpha rhythms and other components of cortical neurodynamics (*15*, *17*, *60*). Our findings indicate that this gene signature is primarily active in both excitatory and inhibitory neurons (Figure 2B). Genetic influences on these cells likely manifest as observable differences in overall brain activity patterns, leading to distinct variations in macroscale brain signaling across individuals.

Conversely, our study revealed that the cortical expression of genes involved in cell morphogenesis and neurogenesis, particularly in limbic regions, exhibits a negative correlation with individual neurophysiological differentiation (Figure 2B). In contrast to positively-loaded genes, which relate to neurochemical interactions between neurons, these negatively-loaded genes are mainly expressed in supportive cells such as astrocytes and microglia. This suggests that genetic influences on neurophysiological individual traits are more related to neuronal communication than to inherited structural brain features, consistent with existing models of the physiological origins of MEG signals(*26*, *43*, *44*).

Our research highlights potential pathways for future studies on individual neurophysiology by providing a biologically grounded framework to understand behavioural variations. Animal models could be instrumental in manipulating alleles of the genes identified in our study to assess their impact on gene product functioning, large-scale brain signal characteristics, and ultimately, behaviour. This approach would provide further insights into how genetic variations influence both neurophysiological traits and behavioural differences.

Our study demonstrates that genetic factors play a significant role in defining the uniqueness of neurophysiological profiles, yet they do not account for all observed variations. While the differentiation accuracy for monozygotic twins is substantial, it does not reach the same level as that for single individuals. This discrepancy suggests an explanatory gap likely attributable to

environmental influences. Environmental factors affect gene expression and behavior(*24*, *61*, *62*) and may also modulate certain neurophysiological traits. The inability to differentiate twin pairs with absolute precision underscores the need for further research with larger twin cohorts to fully elucidate the interplay between genetics and environment in shaping individual brain activity.

Alignment of the Gene-Differentiation Signature with Neuropsychological Processes

We found that, across the cortex, the gene-differentiation signature of neurophysiological profiles aligns with maps of cortical activations related to specific cognitive and emotional processes (Figure 2C). This alignment was pronounced for cognitive functions such as attention and, unexpectedly, for affective processes such as emotion regulation, challenging the traditional separation between cognition and emotions (*63*). This suggests that both cognitive abilities and emotional regulation are linked to gene expression related to neuronal communication. As shown above, genes involved in neuronal communication exhibited the strongest cortical expression alignment with the most differentiating traits of neurophysiological profiles. This linkage between cortical mapping of cognitive abilities and emotional regulation with the gene-differentiation signature supports a more integrated model of neuropsychological processes, bridging cognitive and affective functions.

Our research also highlights the importance of limbic brain regions, including the anterior cingulate cortex (Figure 2C), which are often linked to mental health disorders (*64–67*). We found that limbic regions involved in affective processes are associated with gene expression related to cell morphogenesis, primarily expressed in astrocytes and microglia (Figure 2B & Figure S6). This relationship, indicated by negative gene scores (Figure 2B & C), underscores the potential role of neuron-support cells in mental health. Furthermore, our data suggest that the neurophysiological signals in limbic regions, particularly those related to emotional processes, may not be distinct enough to differentiate individuals effectively (Figure 2A). This insight is particularly relevant for the application of personalized medicine in mental health.

Trajectory of the Neurophysiological Profile Through the Lifespan

We report that the gene-differentiation signature becomes more pronounced with age (Figure 3). This observation aligns with previous neuroimaging studies showing that individual brain-fingerprint features become more stable and unique as people age (*5*, *68*) (Figure 3). It is also consistent with findings that the influence of genetics on cognitive processes increases across the lifespan (*23*, *25*, *48*). Our data demonstrate that while the overall neurophysiological profile becomes more distinct and individualized with age, the specific traits that are most salient can change over the lifespan, paralleling the maturation of cortical gene expression. These findings provide new biological insights into the widely reported changes in neurophysiological brain activity associated with aging (*69–74*).

Methodological Considerations and Future Directions

Previous neuroimaging studies with fMRI have shown how gene expression modulates functional connectivity in the frontoparietal network, a key feature of inter-individual differentiation in fMRI brain-fingerprints (*75*). In contrast, our study highlights the role of posterior unimodal sensory cortical regions in driving inter-individual differentiation based on neurophysiological traits. This disparity between neuroimaging modalities underscores the distinct biological underpinnings of hemodynamic fMRI and electrophysiological signals (*1*, *2*, *50*, *76*). Specifically, while fMRI connectome-based individual profiles partially reflect the structural connections between network nodes (*77*, *78*), our findings indicate that individual neurophysiological profiles are predominantly shaped by processes of neuronal communication, particularly through the expression of genes involved in ion transport and neurotransmission. This distinction underscores the critical role of these genes in mediating neuronal signalling and brain activity patterns, providing novel insight into the mechanisms underlying neurophysiological individuality.

We must also underscore potential limitations in the interpretation of our findings. Heritability estimates were derived using Falconer's formula, which does not account for variance due to environmental factors. As already mentioned above, future studies with larger twin samples and comprehensive documentation of demographics and socioeconomic factors are warranted to address this limitation. Our genomics analysis is based on rare, albeit limited, data from a small sample of post-mortem brain tissue. The tissue sampling process has inherent biases, such as a focus on the left hemisphere and sex imbalance. Future research should aim to mitigate these biases. Additionally, we acknowledge that post-mortem gene expression measures may not accurately reflect in vivo conditions (*79*).

The correlational nature of our findings highlights the need for further experimental validation, potentially through animal models, to establish causative links between gene expression and neurophysiological and behavioural traits. The gene-differentiation signature and its relationship to neuropsychological processes highlighted in our study were derived from meta-analytic findings (*80*). While we believe these findings are novel and biologically meaningful, they do not provide a complete picture of the neural basis of behaviour. The inherent limitations of meta-analytic approaches and the limited scope of behaviours analyzed here will need to be expanded upon in future studies.

In conclusion, our research elucidates the relationship between molecular variations, brain activity, and individual differences. Using a multiscale, data-driven approach, the present study suggests new avenues for understanding the biological foundations of individual variability. Our findings lay the groundwork for future studies to further explore these complex interconnections, thereby enriching our understanding of the neural underpinnings of human behaviour and cognition. We hope that our work will inspire continued exploration and innovation in the field, ultimately advancing our knowledge of how genetic and neurophysiological factors shape the human experience.

Methods:

Participants: MRI and MEG data from 89 healthy young adults (22-35 years old; mean= 28.6, SD= 3.8 years) were collected from the Human Connectome Project (HCP)(*28*). Among these 89 participants, 34 were monozygotic twins, and 22 were dizygotic twins. The zygosity of the participants was confirmed with genotyping tests. All participants underwent three approximately six-minute resting-state eyes-open MEG recordings using a 248-magnetometer whole-head Magnes 3600 system (4DNeuroimaging, San Diego, CA). All sessions were conducted at the same location with a sampling rate of 2034.5 Hz, as detailed in HCP protocols(*28*).

Ethics: The procedures for the curation and analysis were reviewed and approved according to the institutional ethics policies of McGill University 's and the Montreal Neurological Institute's Research Ethics Boards (ref no. 22-06-079).

MEG Data Preprocessing & Source Mapping: MEG data were preprocessed following good practice guidelines(*81*) using Brainstorm(*82*). Source maps for each participant's recordings were computed using a linearly-constrained minimum-variance (LCMV) beamformer and were clustered into 200 cortical parcels of the Schaefer atlas(*83*), as detailed in Supplemental Information Methods.

Neurophysiological Profiles: Power spectrum density (PSD) estimates at each cortical parcel were derived using Welch's method (sliding window of 2 s, 50% overlap). The neurophysiological profile (or *brain-fingerprint*) of each participant consisted of PSD values defined at 301 frequency bins (range: 0-150Hz; ½ Hz resolution) for each of the 200 cortical parcels. Neurophysiological profiles were generated for each of the three MEG recordings per participant.

Individual Differentiation: Individual neurophysiological profiling was conducted following our previous work (Figure 1A)(*2*). We assessed the correlational similarity between participants' neurophysiological profiles across recordings. For each probe participant, we computed Pearson's correlation coefficients between their neurophysiological profile from one their three recordings available and a test set consisting of the neurophysiological profiles of all participants derived from another one of the other two recordings (between-participants similarity), including the probe participant's profile (within-participant similarity). A participant was correctly differentiated if the highest correlation coefficient between their neurophysiological profile and the test set was obtained from their own neurophysiological profile from the other recording. This procedure was repeated for all participants. We then computed the percentage of correctly differentiated participants across the cohort, yielding a score of differentiation accuracy for the neurophysiological profiling approach. This procedure was repeated for all possible pairs of data recordings from the three available for each participant, and the mean differentiation accuracy was reported.

Matching Neurophysiological Profiles Between Twin Pairs: We declared that the neurophysiological profiles of twin siblings matched with one another if their Pearson's correlation coefficients were higher than with any other participant. This matching procedure was repeated for all twin pairs in the cohort, and we reported the percentage of correctly matched pairs separately for monozygotic and dizygotic twin pairs.

Band-limited Neurophysiological Profiles: We replicated the individual and twin pair neurophysiological profiling analyses, restricting the PSD features to those averaged over the typical electrophysiological frequency bands: delta (1–4 Hz), theta (4–8 Hz), alpha (8–13 Hz), beta (13–30 Hz), gamma (30–50 Hz), and high-gamma (50–150 Hz).

Bootstrapping of Differentiation Accuracy Scores: To derive confidence intervals for the reported differentiation accuracies, we employed a bootstrapping method. We randomly selected a subset of participants representing approximately 90% of the tested cohort (i.e., 30 MZ, 20 DZ, and 30 non-twins), derived a differentiation accuracy score, and repeated this procedure 1000 times with random subsamples of participants. We report 95% confidence intervals from the 2.5^{th} and 97.5^{th} percentiles of the resulting empirical distribution of differentiation accuracies. For deriving confidence intervals for the differentiation of twin pairs, we randomly subsampled 15 MZ twin pairs and 10 DZ twin pairs for each iteration of the random subsampling.

Saliency of Neurophysiological Traits: We calculated intraclass correlations (ICC) to quantify the contribution of each cortical parcel and frequency band toward differentiating between individuals across the cohort. ICC quantifies the ratio of within-participant to between-participant variance. High ICC values indicate the saliency of a feature of the neurophysiological profile (a neurophysiological *trait*) in distinguishing individuals, as it reflects high within-participant consistency and low between-participant variability. To avoid potential bias due to twin pairs, we computed ICC across all individuals in the cohort and across 100 random subsamples, ensuring only one twin from each pair was included in each subsample (i.e., for each subsample, we randomly selected either twin A or twin B to include in the calculation of ICC). The ICC values obtained from bootstrapping were nearly identical to those obtained from the entire cohort (98.6% correlation). We proceeded with the ICC values averaged across bootstraps for all analyses.

Heritability of Neurophysiological Traits: We calculated the heritability of individual neurophysiological profiles, considered as phenotypes, using the Falconer formula(*10*). This method estimates the relative contribution of genetics versus environmental factors in determining a phenotype. A phenotype in this context refers to the overall neurophysiological profile of an individual, while a trait refers to specific aspects or features within this profile, such as power spectrum density in a particular frequency band or cortical region. If the similarity in a phenotype between monozygotic (MZ) twins is greater than that between dizygotic (DZ) twins, the trait is considered heritable:

$$H^2 = 2(r_{MZ} - r_{DZ}),$$

where r_{MZ} (and r_{DZ}, respectively) is the intraclass correlation between MZ (and DZ, respectively) twin pairs for a given neurophysiological trait. It is important to note that heritability reflects the similarity within twin pairs for a given phenotype, whereas ICC reflects the stability of a trait within a person relative to others in the cohort.

Gene Expression Data: Gene expression data was obtained from the six postmortem brains provided by the Allen Human Brain Atlas (AHBA; http://human.brain-map.org/)(*33*)using the *abagen* python package(*35*). Our analyses followed a similar pipeline to prior studies(*32*). Gene expression was obtained by averaging across donors. We retained 9104 genes with a differential stability above 0.1 for all future analyses, following good-practice guidelines and previous literature(*32*, *34*, *35*, *84*). See Supplemental Information Methods for further details.

PLS Derivation of a Gene-Differentiation Signature: We related salient features for participant differentiation to gene expression gradients using a partial least squares (PLS)(*85–87*) analysis. We z-scored the columns of two data arrays: one containing the most salient neurophysiological traits (ICC values) and the other containing gene expression levels. The neurophysiological traits array (denoted as *Y*) had 6 columns representing each frequency band of interest and 200 rows representing the cortical parcels of the Schaefer atlas. The gene expression array (denoted as *X*) had 9104 columns representing genes and 200 rows representing the same cortical parcels. We applied singular value decomposition (SVD) to the covariation matrix of *X* and *Y* such that:

$$\mathrm{Cov}(X, Y) = USV^T,$$

where *U* and *V* are the left and right singular vectors, and *S* is the diagonal matrix of singular values. As typical with PLS, this decomposition allowed us to identify the latent variables that maximally covary between the gene expression data and the neurophysiological traits. Each singular value indicates the amount of covariance explained by its corresponding latent component. The vectors *U* and *V* provide the weights for the genes and frequency bands, respectively, for each latent component. High weights in *U* correspond to genes that strongly covary with high weights in *V*, which correspond to specific frequency bands. Positively weighted genes covary with positively weighted frequency bands, elucidating the relationship between genetic and neurophysiological variability.

Gene expression and ICC scores were computed for each cortical parcel by projecting the original data matrices *X* and *Y* onto the singular vector weights obtained from the PLS analysis. Specifically, these scores represent the covariance between the gene expression data and the neurophysiological traits. For example, cortical parcels with positive scores indicate covariance between positively weighted genes and positively weighted frequency bands, which are important for participant differentiation.

Loadings were computed as Pearson's correlation coefficients between each variable's regional spatial distribution over the cortex (i.e., gene expression and ICC data) and the corresponding cortical score pattern (i.e., correlating gene expression with ICC scores). We used Pearson's

correlation coefficients for our loadings because they provide a standardized measure of the strength and direction of the linear relationship between variables, facilitating interpretation. Variables with large absolute loadings are highly correlated with the observed score pattern and strongly relate to the latent component of covariance.

To assess the significance of the latent components, we conducted permutation tests that preserved the spatial autocorrelation of cortical maps (see below). Specifically, we performed 1,000 spin tests and computed a null distribution of singular values. P-values were computed as the proportion of null singular values that achieved a greater magnitude than the empirical singular values. Additionally, we computed bootstrapped confidence intervals for the singular values by randomly resampling the rows (corresponding to the cortical parcels) of both data matrices 1,000 times. We report the 2.5^{th} and 97.5^{th} percentiles of the resulting distribution of singular values.

Gene Ontology Analysis: To determine the biological processes that strongly contributed to the set of positively and negatively loaded genes, we conducted an enrichment analysis using gene ontology(*88*, *89*), a framework for categorizing gene products based on their molecular function and associated biological processes(*36*, *88*).

For negatively and positively loaded genes, we separately selected the 50% with the largest absolute loadings (e.g., genes with the 50% most negative or positive loadings) and input these genes into the *ShinyGO v.0.77* gene ontology tool(*36*) using the GO biological processes pathway databases(*89*). Genes without Enrtez IDs were excluded from the analysis. P-values associated with fold enrichment for all terms were FDR corrected. See Supplemental Data for a comprehensive list of all biological processes and their corresponding fold enrichment values.

Cell-type Deconvolution: We aggregated cell-specific gene sets for seven cell types using data from five human adult postmortem single-cell and single-nucleus RNA sequencing studies(*37–41*, *47*). The seven cell classes were determined based on hierarchical clustering, resulting in the following cell types: astrocytes, endothelial cells, microglia, excitatory neurons, inhibitory neurons, oligodendrocytes, and oligodendrocyte precursor cells (OPC).

We assessed the preferential expression of cell-specific gene sets by 1) computing the ratio of positively loaded genes that overlapped with the cell-specific gene set; and 2) permuting gene sets 1,000 times to assess statistical significance.

This approach allowed us to determine the statistical significance of the overlap between the loaded genes and the cell-specific gene sets, providing insights into the cell-type-specific expression patterns of the genes contributing to the neurophysiological traits.

Gene Expression & Neuropsychological Processes PLS Analysis: We repeated the above-described PLS analysis to relate gene expression to neuropsychological processes, as indexed by brain activation maps obtained from *Neurosynth*(*80*). This analysis replicated the approach of

Hansen and colleagues(*32*), using the Schaefer-200 atlas(*83*). For detailed methodology, see Supplemental Information Methods.

Gene-Signature Evolution Across Developmental Stages: We used brain gene expression data available from BrainSpan(*49*) ,which features gene expression levels from different developmental stages ranging from 8 post-conception weeks to 40 years of age. We computed gene scores for 12 cortical regions across neurodevelopmental stages by multiplying the gene expression matrix obtained from BrainSpan with the PLS-derived gene weights (columns of *U* above).

We fitted linear slopes—using the MATLAB *polyfit()* function—to the gene scores across neurodevelopment for each cortical parcel separately. These slopes were then compared to statistical null slope values obtained by performing spatially autocorrelation-preserving permutations, then running the PLS analysis pipeline, and multiplying the null gene weights with BrainSpan gene expression data. This resulted in a null distribution of slopes (1,000 permutations). See Supplemental Information Methods for further details.

Visualization: We plotted brain maps of ICC, heritability, and PLS brain scores using the *ggSchaefer* and *ggseg* R packages. All other plots were generated using the *ggplot2* package in R(*90*).

Correction for Spatial Autocorrelation of Cortical Maps: We corrected for spatial autocorrelation of cortical map data, where applicable, using SPIN tests. SPIN tests preserve the spatial autocorrelation of cortical topographies by rotating the cortex surface data, effectively permuting the spatial positions while maintaining the spatial structure. This generates a null distribution that accounts for spatial autocorrelation. We conducted 1,000 spin permutations of our brain maps using the Hungarian method(*91*, *92*).

References:

1. E. S. Finn, X. Shen, D. Scheinost, M. D. Rosenberg, J. Huang, M. M. Chun, X. Papademetris, R. T. Constable, Functional connectome fingerprinting: identifying individuals using patterns of brain connectivity. *Nat. Neurosci.* **18**, 1664–1671 (2015).

2. J. da Silva Castanheira, H. D. Orozco Perez, B. Misic, S. Baillet, Brief segments of neurophysiological activity enable individual differentiation. *Nat. Commun.* **12**, 5713 (2021).

3. E. Amico, J. Goñi, The quest for identifiability in human functional connectomes. *Sci. Rep.* **8**, 8254 (2018).

4. T. Kaufmann, D. Alnæs, C. L. Brandt, F. Bettella, S. Djurovic, O. A. Andreassen, L. T. Westlye, Stability of the Brain Functional Connectome Fingerprint in Individuals With Schizophrenia. *JAMA Psychiatry* **75**, 749–751 (2018).

5. T. Kaufmann, D. Alnæs, N. T. Doan, C. L. Brandt, O. A. Andreassen, L. T. Westlye, Delayed stabilization and individualization in connectome development are related to psychiatric disorders. *Nat. Neurosci.* **20**, 513–515 (2017).

6. P. Sorrentino, R. Rucco, A. Lardone, M. Liparoti, E. Troisi Lopez, C. Cavaliere, A. Soricelli, V. Jirsa, G. Sorrentino, E. Amico, Clinical connectome fingerprints of cognitive decline. *NeuroImage* **238**, 118253 (2021).

7. E. Troisi Lopez, R. Minino, M. Liparoti, A. Polverino, A. Romano, R. De Micco, F. Lucidi, A. Tessitore, E. Amico, G. Sorrentino, V. Jirsa, P. Sorrentino, Fading of brain network fingerprint in Parkinson's disease predicts motor clinical impairment. *Hum. Brain Mapp.* **44**, 1239–1250 (2023).

8. J. da Silva Castanheira, A. I. Wiesman, J. Y. Hansen, B. Misic, S. Baillet, J. Breitner, J. Poirier, P. Bellec, V. Bohbot, M. Chakravarty, The neurophysiological brain-fingerprint of Parkinson's disease. *EBioMedicine* **105** (2024).

9. Z. Fu, J. Liu, M. S. Salman, J. Sui, V. D. Calhoun, Functional connectivity uniqueness and variability? Linkages with cognitive and psychiatric problems in children. *Nat. Ment. Health* **1**, 956–970 (2023).

10. D. S. Falconer, The inheritance of liability to certain diseases, estimated from the incidence among relatives. *Ann. Hum. Genet.* **29**, 51–76 (1965).

11. F. Pizzagalli, G. Auzias, Q. Yang, S. R. Mathias, J. Faskowitz, J. D. Boyd, A. Amini, D. Rivière, K. L. McMahon, G. I. de Zubicaray, N. G. Martin, J.-F. Mangin, D. C. Glahn, J. Blangero, M. J. Wright, P. M. Thompson, P. Kochunov, N. Jahanshad, The reliability and heritability of cortical folds and their genetic correlations across hemispheres. *Commun. Biol.* **3**, 1–12 (2020).

12. D. Posthuma, E. J. C. de Geus, E. J. C. M. Mulder, D. J. A. Smit, D. I. Boomsma, C. J. Stam, Genetic components of functional connectivity in the brain: The heritability of synchronization likelihood. *Hum. Brain Mapp.* **26**, 191–198 (2005).

13. J. E. Schmitt, A. Raznahan, S. Liu, M. C. Neale, The Heritability of Cortical Folding: Evidence from the Human Connectome Project. *Cereb. Cortex N. Y. NY* **31**, 702–715 (2020).

14. P. H. Lee, J. T. Baker, A. J. Holmes, N. Jahanshad, T. Ge, J.-Y. Jung, Y. Cruz, D. S. Manoach, D. P. Hibar, J. Faskowitz, K. L. McMahon, G. I. de Zubicaray, N. H. Martin, M. J. Wright, D. Öngür, R. Buckner, J. Roffman, P. M. Thompson, J. W. Smoller, Partitioning heritability analysis reveals a shared genetic basis of brain anatomy and schizophrenia. *Mol. Psychiatry* **21**, 1680–1689 (2016).

15. C. M. Smit, M. J. Wright, N. K. Hansell, G. M. Geffen, N. G. Martin, Genetic variation of individual alpha frequency (IAF) and alpha power in a large adolescent twin sample. *Int. J. Psychophysiol. Off. J. Int. Organ. Psychophysiol.* **61**, 235–243 (2006).

16. E. Salmela, H. Renvall, J. Kujala, O. Hakosalo, M. Illman, M. Vihla, E. Leinonen, R. Salmelin, J. Kere, Evidence for genetic regulation of the human parieto-occipital 10-Hz rhythmic activity. *Eur. J. Neurosci.* **44**, 1963–1971 (2016).

17. B. P. Zietsch, J. L. Hansen, N. K. Hansell, G. M. Geffen, N. G. Martin, M. J. Wright, Common and specific genetic influences on EEG power bands delta, theta, alpha, and beta. *Biol. Psychol.* **75**, 154–164 (2007).

18. R. F. Betzel, J. D. Medaglia, A. E. Kahn, J. Soffer, D. R. Schonhaut, D. S. Bassett, Structural, geometric and genetic factors predict interregional brain connectivity patterns probed by electrocorticography. *Nat. Biomed. Eng.* **3**, 902–916 (2019).

19. J. Richiardi, A. Altmann, A.-C. Milazzo, C. Chang, M. M. Chakravarty, T. Banaschewski, G. J. Barker, A. L. W. Bokde, U. Bromberg, C. Büchel, P. Conrod, M. Fauth-Bühler, H. Flor, V. Frouin, J. Gallinat, H. Garavan, P. Gowland, A. Heinz, H. Lemaître, K. F. Mann, J.-L. Martinot, F. Nees, T. Paus, Z. Pausova, M. Rietschel, T. W. Robbins, M. N. Smolka, R. Spanagel, A. Ströhle, G. Schumann, M. Hawrylycz, J.-B. Poline, M. D. Greicius, IMAGEN CONSORTIUM, Correlated gene expression supports synchronous activity in brain networks. *Science* **348**, 1241–1244 (2015).

20. B. D. Fulcher, J. D. Murray, V. Zerbi, X.-J. Wang, Multimodal gradients across mouse cortex. *Proc. Natl. Acad. Sci.* **116**, 4689–4695 (2019).

21. I. Zwir, J. Arnedo, C. Del-Val, L. Pulkki-Råback, B. Konte, S. S. Yang, R. Romero-Zaliz, M. Hintsanen, K. M. Cloninger, D. Garcia, D. M. Svrakic, S. Rozsa, M. Martinez, L.-P. Lyytikäinen, I. Giegling, M. Kähönen, H. Hernandez-Cuervo, I. Seppälä, E. Raitoharju, G. A. de Erausquin, O. Raitakari, D. Rujescu, T. T. Postolache, J. Sung, L. Keltikangas-Järvinen, T. Lehtimäki, C. R. Cloninger, Uncovering the complex genetics of human character. *Mol. Psychiatry* **25**, 2295–2312 (2020).

22. R. A. Power, M. Pluess, Heritability estimates of the Big Five personality traits based on common genetic variants. *Transl. Psychiatry* **5**, e604 (2015).

23. J. Mollon, E. E. M. Knowles, S. R. Mathias, R. Gur, J. M. Peralta, D. J. Weiner, E. B. Robinson, R. E. Gur, J. Blangero, L. Almasy, D. C. Glahn, Genetic influence on cognitive development between childhood and adulthood. *Mol. Psychiatry* **26**, 656–665 (2021).

24. T. J. Bouchard, M. McGue, Genetic and environmental influences on human psychological differences. *J. Neurobiol.* **54**, 4–45 (2003).

25. C. Haworth, M. Wright, M. Luciano, N. Martin, E. de Geus, C. van Beijsterveldt, M. Bartels, D. Posthuma, D. Boomsma, O. Davis, Y. Kovas, R. Corley, J. DeFries, J. Hewitt, R. Olson, S.-A. Rhea, S. Wadsworth, W. Iacono, M. McGue, L. Thompson, S. Hart, S. Petrill, D. Lubinski, R. Plomin, The heritability of general cognitive ability increases linearly from childhood to young adulthood. *Mol. Psychiatry* **15**, 1112–1120 (2010).

26. S. Baillet, Magnetoencephalography for brain electrophysiology and imaging. *Nat. Neurosci.* **20**, 327–339 (2017).

27. A. J. Mayhew, D. Meyre, Assessing the Heritability of Complex Traits in Humans: Methodological Challenges and Opportunities. *Curr. Genomics* **18**, 332–340 (2017).

28. D. C. Van Essen, K. Ugurbil, E. Auerbach, D. Barch, T. E. J. Behrens, R. Bucholz, A. Chang, L. Chen, M. Corbetta, S. W. Curtiss, S. Della Penna, D. Feinberg, M. F. Glasser, N. Harel, A. C. Heath, L. Larson-Prior, D. Marcus, G. Michalareas, S. Moeller, R. Oostenveld, S. E. Petersen, F. Prior, B. L. Schlaggar, S. M. Smith, A. Z. Snyder, J. Xu, E. Yacoub, The Human Connectome Project: A data acquisition perspective. *NeuroImage* **62**, 2222–2231 (2012).

29. J. da Silva Castanheira, A. I. Wiesman, J. Y. Hansen, B. Misic, S. Baillet, PREVENT-AD Research Group, Quebec Parkinson Network, Neurophysiological brain-fingerprints of motor and cognitive decline in Parkinson's disease. *MedRxiv Prepr. Serv. Health Sci.*, 2023.02.03.23285441 (2023).

30. B. T. T. Yeo, F. M. Krienen, J. Sepulcre, M. R. Sabuncu, D. Lashkari, M. Hollinshead, J. L. Roffman, J. W. Smoller, L. Zöllei, J. R. Polimeni, B. Fischl, H. Liu, R. L. Buckner, The organization of the human cerebral cortex estimated by intrinsic functional connectivity. *J. Neurophysiol.* **106**, 1125–1165 (2011).

31. J. B. Burt, M. Demirtaş, W. J. Eckner, N. M. Navejar, J. L. Ji, W. J. Martin, A. Bernacchia, A. Anticevic, J. D. Murray, Hierarchy of transcriptomic specialization across human cortex captured by structural neuroimaging topography. *Nat. Neurosci.* **21**, 1251–1259 (2018).

32. J. Y. Hansen, R. D. Markello, J. W. Vogel, J. Seidlitz, D. Bzdok, B. Misic, Mapping gene transcription and neurocognition across human neocortex. *Nat. Hum. Behav.* **5**, 1240–1250 (2021).

33. M. J. Hawrylycz, E. S. Lein, A. L. Guillozet-Bongaarts, E. H. Shen, L. Ng, J. A. Miller, L. N. van de Lagemaat, K. A. Smith, A. Ebbert, Z. L. Riley, C. Abajian, C. F. Beckmann, A. Bernard, D. Bertagnolli, A. F. Boe, P. M. Cartagena, M. M. Chakravarty, M. Chapin, J. Chong, R. A. Dalley, B. D. Daly, C. Dang, S. Datta, N. Dee, T. A. Dolbeare, V. Faber, D. Feng, D. R. Fowler, J. Goldy, B. W. Gregor, Z. Haradon, D. R. Haynor, J. G. Hohmann, S. Horvath, R. E. Howard, A. Jeromin, J. M. Jochim, M. Kinnunen, C. Lau, E. T. Lazarz, C. Lee, T. A. Lemon, L. Li, Y. Li, J. A. Morris, C. C. Overly, P. D. Parker, S. E. Parry, M. Reding, J. J. Royall, J. Schulkin, P. A. Sequeira, C. R. Slaughterbeck, S. C. Smith, A. J. Sodt, S. M. Sunkin, B. E. Swanson, M. P. Vawter, D. Williams, P. Wohnoutka, H. R. Zielke, D. H. Geschwind, P. R. Hof, S. M. Smith, C. Koch, S. G. N. Grant, A. R. Jones, An anatomically comprehensive atlas of the adult human brain transcriptome. *Nature* **489**, 391–399 (2012).

34. M. Hawrylycz, J. A. Miller, V. Menon, D. Feng, T. Dolbeare, A. L. Guillozet-Bongaarts, A. G. Jegga, B. J. Aronow, C.-K. Lee, A. Bernard, M. F. Glasser, D. L. Dierker, J. Menche, A. Szafer, F. Collman, P. Grange, K. A. Berman, S. Mihalas, Z. Yao, L. Stewart, A.-L. Barabási, J.

Schulkin, J. Phillips, L. Ng, C. Dang, D. R. Haynor, A. Jones, D. C. Van Essen, C. Koch, E. Lein, Canonical genetic signatures of the adult human brain. *Nat. Neurosci.* **18**, 1832–1844 (2015).

35. R. D. Markello, A. Arnatkeviciute, J.-B. Poline, B. D. Fulcher, A. Fornito, B. Misic, Standardizing workflows in imaging transcriptomics with the abagen toolbox. *eLife* **10**, e72129 (2021).

36. S. X. Ge, D. Jung, R. Yao, ShinyGO: a graphical gene-set enrichment tool for animals and plants. *Bioinformatics* **36**, 2628–2629 (2020).

37. Y. Zhang, S. A. Sloan, L. E. Clarke, C. Caneda, C. A. Plaza, P. D. Blumenthal, H. Vogel, G. K. Steinberg, M. S. B. Edwards, G. Li, J. A. Duncan, S. H. Cheshier, L. M. Shuer, E. F. Chang, G. A. Grant, M. G. H. Gephart, B. A. Barres, Purification and Characterization of Progenitor and Mature Human Astrocytes Reveals Transcriptional and Functional Differences with Mouse. *Neuron* **89**, 37–53 (2016).

38. B. B. Lake, S. Chen, B. C. Sos, J. Fan, G. E. Kaeser, Y. C. Yung, T. E. Duong, D. Gao, J. Chun, P. V. Kharchenko, K. Zhang, Integrative single-cell analysis of transcriptional and epigenetic states in the human adult brain. *Nat. Biotechnol.* **36**, 70–80 (2018).

39. N. Habib, I. Avraham-Davidi, A. Basu, T. Burks, K. Shekhar, M. Hofree, S. R. Choudhury, F. Aguet, E. Gelfand, K. Ardlie, D. A. Weitz, O. Rozenblatt-Rosen, F. Zhang, A. Regev, Massively parallel single-nucleus RNA-seq with DroNc-seq. *Nat. Methods* **14**, 955–958 (2017).

40. S. Darmanis, S. A. Sloan, Y. Zhang, M. Enge, C. Caneda, L. M. Shuer, M. G. Hayden Gephart, B. A. Barres, S. R. Quake, A survey of human brain transcriptome diversity at the single cell level. *Proc. Natl. Acad. Sci.* **112**, 7285–7290 (2015).

41. M. Li, G. Santpere, Y. Imamura Kawasawa, O. V. Evgrafov, F. O. Gulden, S. Pochareddy, S. M. Sunkin, Z. Li, Y. Shin, Y. Zhu, A. M. M. Sousa, D. M. Werling, R. R. Kitchen, H. J. Kang, M. Pletikos, J. Choi, S. Muchnik, X. Xu, D. Wang, B. Lorente-Galdos, S. Liu, P. Giusti-Rodríguez, H. Won, C. A. de Leeuw, A. F. Pardiñas, BrainSpan Consortium, PsychENCODE Consortium, PsychENCODE Developmental Subgroup, M. Hu, F. Jin, Y. Li, M. J. Owen, M. C. O'Donovan, J. T. R. Walters, D. Posthuma, M. A. Reimers, P. Levitt, D. R. Weinberger, T. M. Hyde, J. E. Kleinman, D. H. Geschwind, M. J. Hawrylycz, M. W. State, S. J. Sanders, P. F. Sullivan, M. B. Gerstein, E. S. Lein, J. A. Knowles, N. Sestan, Integrative functional genomic analysis of human brain development and neuropsychiatric risks. *Science* **362**, eaat7615 (2018).

42. A. T. McKenzie, M. Wang, M. E. Hauberg, J. F. Fullard, A. Kozlenkov, A. Keenan, Y. L. Hurd, S. Dracheva, P. Casaccia, P. Roussos, B. Zhang, Brain Cell Type Specific Gene Expression and Co-expression Network Architectures. *Sci. Rep.* **8**, 8868 (2018).

43. S. Baillet, J. C. Mosher, R. M. Leahy, Electromagnetic brain mapping. *IEEE Signal Process. Mag.* **18**, 14–30 (2001).

44. M. Hämäläinen, R. Hari, R. J. Ilmoniemi, J. Knuutila, O. V. Lounasmaa, Magnetoencephalography---theory, instrumentation, and applications to noninvasive studies of the working human brain. *Rev. Mod. Phys.* **65**, 413–497 (1993).

45. M. D. Rosenberg, E. S. Finn, D. Scheinost, R. T. Constable, M. M. Chun, Characterizing Attention with Predictive Network Models. *Trends Cogn. Sci.* **21**, 290–302 (2017).

46. M. D. Rosenberg, D. Scheinost, A. S. Greene, E. W. Avery, Y. H. Kwon, E. S. Finn, R. Ramani, M. Qiu, R. T. Constable, M. M. Chun, Functional connectivity predicts changes in attention observed across minutes, days, and months. *Proc. Natl. Acad. Sci.* **117**, 3797–3807 (2020).

47. J. Seidlitz, A. Nadig, S. Liu, R. A. I. Bethlehem, P. E. Vértes, S. E. Morgan, F. Váša, R. Romero-Garcia, F. M. Lalonde, L. S. Clasen, J. D. Blumenthal, C. Paquola, B. Bernhardt, K. Wagstyl, D. Polioudakis, L. de la Torre-Ubieta, D. H. Geschwind, J. C. Han, N. R. Lee, D. G. Murphy, E. T. Bullmore, A. Raznahan, Transcriptomic and cellular decoding of regional brain vulnerability to neurogenetic disorders. *Nat. Commun.* **11**, 3358 (2020).

48. D. A. Briley, E. M. Tucker-Drob, Comparing the Developmental Genetics of Cognition and Personality over the Lifespan. *J. Pers.* **85**, 51–64 (2017).

49. J. A. Miller, S.-L. Ding, S. M. Sunkin, K. A. Smith, L. Ng, A. Szafer, A. Ebbert, Z. L. Riley, J. J. Royall, K. Aiona, J. M. Arnold, C. Bennet, D. Bertagnolli, K. Brouner, S. Butler, S. Caldejon, A. Carey, C. Cuhaciyan, R. A. Dalley, N. Dee, T. A. Dolbeare, B. A. C. Facer, D. Feng, T. P. Fliss, G. Gee, J. Goldy, L. Gourley, B. W. Gregor, G. Gu, R. E. Howard, J. M. Jochim, C. L. Kuan, C. Lau, C.-K. Lee, F. Lee, T. A. Lemon, P. Lesnar, B. McMurray, N. Mastan, N. Mosqueda, T. Naluai-Cecchini, N.-K. Ngo, J. Nyhus, A. Oldre, E. Olson, J. Parente, P. D. Parker, S. E. Parry, A. Stevens, M. Pletikos, M. Reding, K. Roll, D. Sandman, M. Sarreal, S. Shapouri, N. V. Shapovalova, E. H. Shen, N. Sjoquist, C. R. Slaughterbeck, M. Smith, A. J. Sodt, D. Williams, L. Zöllei, B. Fischl, M. B. Gerstein, D. H. Geschwind, I. A. Glass, M. J. Hawrylycz, R. F. Hevner, H. Huang, A. R. Jones, J. A. Knowles, P. Levitt, J. W. Phillips, N. Šestan, P. Wohnoutka, C. Dang, A. Bernard, J. G. Hohmann, E. S. Lein, Transcriptional landscape of the prenatal human brain. *Nature* **508**, 199–206 (2014).

50. E. Sareen, S. Zahar, D. V. D. Ville, A. Gupta, A. Griffa, E. Amico, Exploring MEG brain fingerprints: Evaluation, pitfalls, and interpretations. *NeuroImage* **240**, 118331 (2021).

51. F. M. Krienen, B. T. T. Yeo, T. Ge, R. L. Buckner, C. C. Sherwood, Transcriptional profiles of supragranular-enriched genes associate with corticocortical network architecture in the human brain. *Proc. Natl. Acad. Sci.* **113**, E469–E478 (2016).

52. B. D. Fulcher, A. Fornito, A transcriptional signature of hub connectivity in the mouse connectome. *Proc. Natl. Acad. Sci.* **113**, 1435–1440 (2016).

53. K. J. Whitaker, P. E. Vértes, R. Romero-Garcia, F. Váša, M. Moutoussis, G. Prabhu, N. Weiskopf, M. F. Callaghan, K. Wagstyl, T. Rittman, R. Tait, C. Ooi, J. Suckling, B. Inkster, P. Fonagy, R. J. Dolan, P. B. Jones, I. M. Goodyer, the NSPN Consortium, E. T. Bullmore, Adolescence is associated with genomically patterned consolidation of the hubs of the human brain connectome. *Proc. Natl. Acad. Sci.* **113**, 9105–9110 (2016).

54. A. F. Alexander-Bloch, A. Raznahan, S. N. Vandekar, J. Seidlitz, Z. Lu, S. R. Mathias, E. Knowles, J. Mollon, A. Rodrigue, J. E. Curran, H. H. H. Görring, T. D. Satterthwaite, R. E. Gur, D. S. Bassett, G. D. Hoftman, G. Pearlson, R. T. Shinohara, S. Liu, P. T. Fox, L. Almasy, J. Blangero, D. C. Glahn, Imaging local genetic influences on cortical folding. *Proc. Natl. Acad. Sci.* **117**, 7430–7436 (2020).

55. R. D. Markello, J. Y. Hansen, Z.-Q. Liu, V. Bazinet, G. Shafiei, L. E. Suárez, N. Blostein, J. Seidlitz, S. Baillet, T. D. Satterthwaite, M. M. Chakravarty, A. Raznahan, B. Misic, neuromaps: structural and functional interpretation of brain maps. *Nat. Methods* **19**, 1472–1479 (2022).

56. Y. Fu, Z. Ma, C. Hamilton, Z. Liang, X. Hou, X. Ma, X. Hu, Q. He, W. Deng, Y. Wang, L. Zhao, H. Meng, T. Li, N. Zhang, Genetic influences on resting-state functional networks: *A twin study*: Genetic Influences on Resting-State Functional Networks. *Hum. Brain Mapp.* **36**, 3959–3972 (2015).

57. A. Fornito, A. Zalesky, D. S. Bassett, D. Meunier, I. Ellison-Wright, M. Yucel, S. J. Wood, K. Shaw, J. O'Connor, D. Nertney, B. J. Mowry, C. Pantelis, E. T. Bullmore, Genetic Influences on Cost-Efficient Organization of Human Cortical Functional Networks. *J. Neurosci.* **31**, 3261–3270 (2011).

58. S. Bodenmann, T. Rusterholz, R. Dürr, C. Stoll, V. Bachmann, E. Geissler, K. Jaggi-Schwarz, H.-P. Landolt, The Functional Val158Met Polymorphism of COMT Predicts Interindividual Differences in Brain α Oscillations in Young Men. *J. Neurosci.* **29**, 10855–10862 (2009).

59. J. V. Rétey, M. Adam, E. Honegger, R. Khatami, U. F. O. Luhmann, H. H. Jung, W. Berger, H.-P. Landolt, A functional genetic variation of adenosine deaminase affects the duration and intensity of deep sleep in humans. *Proc. Natl. Acad. Sci.* **102**, 15676–15681 (2005).

60. G. Winterer, R. Mahlberg, M. N. Smolka, J. Samochowiec, M. Ziller, H.-P. Rommelspacher, W. M. Herrmann, L. G. Schmidt, T. Sander, Association Analysis of Exonic Variants of the GABAB-Receptor Gene and Alpha Electroencephalogram Voltage in Normal Subjects and Alcohol-Dependent Patients. *Behav. Genet.* **33**, 7–15 (2003).

61. M. J. Meaney, A. C. Ferguson-Smith, Epigenetic regulation of the neural transcriptome: the meaning of the marks. *Nat. Neurosci.* **13**, 1313–1318 (2010).

62. S. J. Virolainen, A. VonHandorf, K. C. M. F. Viel, M. T. Weirauch, L. C. Kottyan, Gene–environment interactions and their impact on human health. *Genes Immun.* **24**, 1–11 (2023).

63. S. Duncan, L. F. Barrett, Affect is a form of cognition: A neurobiological analysis. *Cogn. Emot.* **21**, 1184–1211 (2007).

64. G. Shafiei, R. D. Markello, C. Makowski, A. Talpalaru, M. Kirschner, G. A. Devenyi, E. Guma, P. Hagmann, N. R. Cashman, M. Lepage, M. M. Chakravarty, A. Dagher, B. Mišić, Spatial Patterning of Tissue Volume Loss in Schizophrenia Reflects Brain Network Architecture. *Biol. Psychiatry* **87**, 727–735 (2020).

65. G. Bush, P. Luu, M. I. Posner, Cognitive and emotional influences in anterior cingulate cortex. *Trends Cogn. Sci.* **4**, 215–222 (2000).

66. M. Goodkind, S. B. Eickhoff, D. J. Oathes, Y. Jiang, A. Chang, L. B. Jones-Hagata, B. N. Ortega, Y. V. Zaiko, E. L. Roach, M. S. Korgaonkar, S. M. Grieve, I. Galatzer-Levy, P. T. Fox, A. Etkin, Identification of a common neurobiological substrate for mental illness. *JAMA Psychiatry* **72**, 305–315 (2015).

67. A. Tanti, C. Belliveau, C. Nagy, M. Maitra, F. Denux, K. Perlman, F. Chen, R. Mpai, C. Canonne, S. Théberge, A. McFarquhar, M. A. Davoli, C. Belzung, G. Turecki, N. Mechawar, Child abuse associates with increased recruitment of perineuronal nets in the ventromedial prefrontal cortex: a possible implication of oligodendrocyte progenitor cells. *Mol. Psychiatry* **27**, 1552–1561 (2022).

68. T. Kaufmann, D. Alnæs, C. L. Brandt, F. Bettella, S. Djurovic, O. A. Andreassen, L. T. Westlye, Stability of the Brain Functional Connectome Fingerprint in Individuals With Schizophrenia. *JAMA Psychiatry* **75**, 749–751 (2018).

69. K. Thuwal, A. Banerjee, D. Roy, Aperiodic and Periodic Components of Ongoing Oscillatory Brain Dynamics Link Distinct Functional Aspects of Cognition across Adult Lifespan. *eNeuro* **8**, ENEURO.0224-21.2021 (2021).

70. B. Voytek, M. A. Kramer, J. Case, K. Q. Lepage, Z. R. Tempesta, R. T. Knight, A. Gazzaley, Age-Related Changes in 1/f Neural Electrophysiological Noise. *J. Neurosci.* **35**, 13257–13265 (2015).

71. B. Voytek, R. T. Knight, Dynamic Network Communication as a Unifying Neural Basis for Cognition, Development, Aging, and Disease. *Biol. Psychiatry* **77**, 1089–1097 (2015).

72. C.-H. Cheng, P.-Y. S. Chan, S. Baillet, Y.-Y. Lin, Age-Related Reduced Somatosensory Gating Is Associated with Altered Alpha Frequency Desynchronization. *Neural Plast.* **2015**, e302878 (2015).

73. T. Hinault, S. Baillet, S. M. Courtney, Age-related changes of deep-brain neurophysiological activity. *Cereb. Cortex N. Y. N 1991* **33**, 3960–3968 (2023).

74. A. Merkin, S. Sghirripa, L. Graetz, A. E. Smith, B. Hordacre, R. Harris, J. Pitcher, J. Semmler, N. C. Rogasch, M. Goldsworthy, Do age-related differences in aperiodic neural activity explain differences in resting EEG alpha? *Neurobiol. Aging* **121**, 78–87 (2023).

75. L. Li, Y. Wei, J. Zhang, J. Ma, Y. Yi, Y. Gu, L. M. W. Li, Y. Lin, Z. Dai, Gene expression associated with individual variability in intrinsic functional connectivity. *NeuroImage* **245**, 118743 (2021).

76. G. Shafiei, S. Baillet, B. Misic, Human electromagnetic and haemodynamic networks systematically converge in unimodal cortex and diverge in transmodal cortex. *PLoS Biol.* **20**, e3001735 (2022).

77. J. C. Pang, K. M. Aquino, M. Oldehinkel, P. A. Robinson, B. D. Fulcher, M. Breakspear, A. Fornito, Geometric constraints on human brain function. *Nature* **618**, 566–574 (2023).

78. T. Sarwar, Y. Tian, B. T. T. Yeo, K. Ramamohanarao, A. Zalesky, Structure-function coupling in the human connectome: A machine learning approach. *NeuroImage* **226**, 117609 (2021).

79. L. E. Liharska, Y. J. Park, K. Ziafat, L. Wilkins, H. Silk, L. M. Linares, R. C. Thompson, E. Vornholt, B. Sullivan, V. Cohen, P. Kota, C. Feng, E. Cheng, J. S. Johnson, M.-K. Rieder, J. Huang, J. Scarpa, J. Polanco, E. Moya, A. Hashemi, M. A. Levin, G. N. Nadkarni, R. Sebra, J. Crary, E. E. Schadt, N. D. Beckmann, B. H. Kopell, A. W. Charney, A study of gene expression in the living human brain. medRxiv [Preprint] (2023). https://doi.org/10.1101/2023.04.21.23288916.

80. T. Yarkoni, R. A. Poldrack, T. E. Nichols, D. C. Van Essen, T. D. Wager, Large-scale automated synthesis of human functional neuroimaging data. *Nat. Methods* **8**, 665–670 (2011).

81. J. Gross, S. Baillet, G. R. Barnes, R. N. Henson, A. Hillebrand, O. Jensen, K. Jerbi, V. Litvak, B. Maess, R. Oostenveld, L. Parkkonen, J. R. Taylor, V. van Wassenhove, M. Wibral, J.-M. Schoffelen, Good practice for conducting and reporting MEG research. *NeuroImage* **65**, 349–363 (2013).

82. F. Tadel, S. Baillet, J. C. Mosher, D. Pantazis, R. M. Leahy, Brainstorm: A User-Friendly Application for MEG/EEG Analysis. *Comput. Intell. Neurosci.* **2011**, 1–13 (2011).

83. A. Schaefer, R. Kong, E. M. Gordon, T. O. Laumann, X.-N. Zuo, A. J. Holmes, S. B. Eickhoff, B. T. T. Yeo, Local-Global Parcellation of the Human Cerebral Cortex from Intrinsic Functional Connectivity MRI. *Cereb. Cortex* **28**, 3095–3114 (2018).

84. A. Arnatkevičiūtė, B. D. Fulcher, A. Fornito, A practical guide to linking brain-wide gene expression and neuroimaging data. *NeuroImage* **189**, 353–367 (2019).

85. A. Krishnan, L. J. Williams, A. R. McIntosh, H. Abdi, Partial Least Squares (PLS) methods for neuroimaging: a tutorial and review. *NeuroImage* **56**, 455–475 (2011).

86. A. R. McIntosh, B. Mišić, Multivariate statistical analyses for neuroimaging data. *Annu. Rev. Psychol.* **64**, 499–525 (2013).

87. A. R. McIntosh, F. L. Bookstein, J. V. Haxby, C. L. Grady, Spatial pattern analysis of functional brain images using partial least squares. *NeuroImage* **3**, 143–157 (1996).

88. M. Ashburner, C. A. Ball, J. A. Blake, D. Botstein, H. Butler, J. M. Cherry, A. P. Davis, K. Dolinski, S. S. Dwight, J. T. Eppig, M. A. Harris, D. P. Hill, L. Issel-Tarver, A. Kasarskis, S. Lewis, J. C. Matese, J. E. Richardson, M. Ringwald, G. M. Rubin, G. Sherlock, Gene Ontology: tool for the unification of biology. *Nat. Genet.* **25**, 25–29 (2000).

89. P. D. Thomas, The Gene Ontology and the meaning of biological function. *Methods Mol. Biol. Clifton NJ* **1446**, 15 (2017).

90. R Core Team, *R: A Language and Environment for Statistical Computing* (R Foundation for Statistical Computing, Vienna, Austria, 2022; https://www.R-project.org/).

91. R. D. Markello, B. Misic, Comparing spatial null models for brain maps. *NeuroImage* **236**, 118052 (2021).

92. F. Váša, B. Mišić, Null models in network neuroscience. *Nat. Rev. Neurosci.* **23**, 493–504 (2022).

93. B. Fischl, FreeSurfer. *NeuroImage* **62**, 774–781 (2012).

94. R. A. Poldrack, A. Kittur, D. Kalar, E. Miller, C. Seppa, Y. Gil, D. S. Parker, F. W. Sabb, R. M. Bilder, The Cognitive Atlas: Toward a Knowledge Foundation for Cognitive Neuroscience. *Front. Neuroinformatics* **5**, 17 (2011).

95. D. M. Werling, S. Pochareddy, J. Choi, J.-Y. An, B. Sheppard, M. Peng, Z. Li, C. Dastmalchi, G. Santpere, A. M. M. Sousa, A. T. N. Tebbenkamp, N. Kaur, F. O. Gulden, M. S. Breen, L. Liang, M. C. Gilson, X. Zhao, S. Dong, L. Klei, A. E. Cicek, J. D. Buxbaum, H. Adle-Biassette, J.-L. Thomas, K. A. Aldinger, D. R. O'Day, I. A. Glass, N. A. Zaitlen, M. E. Talkowski, K. Roeder, M. W. State, B. Devlin, S. J. Sanders, N. Sestan, Whole-Genome and RNA Sequencing Reveal Variation and Transcriptomic Coordination in the Developing Human Prefrontal Cortex. *Cell Rep.* **31**, 107489 (2020).

96. Y. Wei, S. C. de Lange, L. H. Scholtens, K. Watanabe, D. J. Ardesch, P. R. Jansen, J. E. Savage, L. Li, T. M. Preuss, J. K. Rilling, D. Posthuma, M. P. van den Heuvel, Genetic mapping and evolutionary analysis of human-expanded cognitive networks. *Nat. Commun.* **10**, 4839 (2019).

97. M. Guardiola-Ripoll, M. Fatjó-Vilas, A Systematic Review of the Human Accelerated Regions in Schizophrenia and Related Disorders: Where the Evolutionary and Neurodevelopmental Hypotheses Converge. *Int. J. Mol. Sci.* **24**, 3597 (2023).

98. K. M. Girskis, A. B. Stergachis, E. M. DeGennaro, R. N. Doan, X. Qian, M. B. Johnson, P. P. Wang, G. M. Sejourne, M. A. Nagy, E. A. Pollina, A. M. M. Sousa, T. Shin, C. J. Kenny, J. L. Scotellaro, B. M. Debo, D. M. Gonzalez, L. M. Rento, R. C. Yeh, J. H. T. Song, M. Beaudin, J. Fan, P. V. Kharchenko, N. Sestan, M. E. Greenberg, C. A. Walsh, Rewiring of human neurodevelopmental gene regulatory programs by human accelerated regions. *Neuron* **109**, 3239-3251.e7 (2021).

99. S. L. W. Driessens, A. A. Galakhova, D. B. Heyer, I. J. Pieterse, R. Wilbers, E. J. Mertens, F. Waleboer, T. S. Heistek, L. Coenen, J. R. Meijer, S. Idema, P. C. De Witt Hamer, D. P. Noske, C. P. J. De Kock, B. R. Lee, K. Smith, J. T. Ting, E. S. Lein, H. D. Mansvelder, N. A. Goriounova, Genes associated with cognitive ability and HAR show overlapping expression patterns in human cortical neuron types. *Nat. Commun.* **14**, 4188 (2023).

100. R. N. Doan, B.-I. Bae, B. Cubelos, C. Chang, A. A. Hossain, S. Al-Saad, N. M. Mukaddes, O. Oner, M. Al-Saffar, S. Balkhy, G. G. Gascon, M. Nieto, C. A. Walsh, Mutations in Human Accelerated Regions Disrupt Cognition and Social Behavior. *Cell* **167**, 341-354.e12 (2016).

101. A. I. Luppi, P. A. M. Mediano, F. E. Rosas, N. Holland, T. D. Fryer, J. T. O'Brien, J. B. Rowe, D. K. Menon, D. Bor, E. A. Stamatakis, A synergistic core for human brain evolution and cognition. *Nat. Neurosci.* **25**, 771–782 (2022).

Acknowledgements:

The funders had no role in study design, data collection and analysis, decision to publish, or preparation of the manuscript. The Brainstorm app is supported by funding to SB from the NIH (R01-EB026299), a Discovery grant from the Natural Science and Engineering Research Council of Canada (436355-13), the CIHR Canada Research Chair in Neural Dynamics of Brain Systems, the Brain Canada Foundation with support from Health Canada, and the Innovative Ideas program from the Canada First Research Excellence Fund, awarded to McGill University for the HBHL initiative. This work was supported by a doctoral fellowship from NSERC (JDSC, JYH).

Author Contribution:

Conceptualization: JDSC, SB
Data Curation: JDSC, JYH
Methodology: JDSC, JP, JYH, BM, SB
Software: JDSC, JP, JYH
Visualization: JDSC, JP
Funding acquisition: SB
Writing – original draft: JDSC, SB
Writing – review & editing: JDSC, JP, JYH, BM, SB

Competing interests:

All authors declare no competing conflicts of interest. The listed funding sources in the Acknowledgements did not play any role in the writing of the manuscript or the decision to submit this manuscript for publication

Data and materials availability:

The data are available through the Human Connectome Project (HCP) repository (https://www.humanconnectome.org/study/hcp-young-adult). Gene expression data are available through the Allan Human Brain atlas (ABHA; http://human.brain-map.org/). The Neurosynth database is available at https://neurosynth.org/.

All in-house code used for data analysis and visualization is available on GitHub https://github.com/Epideixx/Fingerprints_Twins.

Supplemental Materials:

Methods (Cont'd.)

MEG data preprocessing. MEG data were preprocessed following good practice guidelines(*81*) using *Brainstorm*(*82*) March-2023 distribution running MATLAB 2020b (Mathworks Inc., Massachusetts, USA). Our preprocessing pipeline was adapted from previous published work(*2*, *29*). Line noise artifacts (60Hz) along with their first 9 harmonics were removed using notch filters. Slow-wave and DC artifacts were attenuated with a high-pass FIR filter above 0.3 Hz. To remove ocular and cardiac physiological artifacts, we defined Signal-Space Projections (SSPs) based on the activity of concurrent electro-cardiogram and -oculogram recordings. We additionally attenuated low-frequency eye saccades (1-7 Hz) and high-frequency (40-240 Hz) muscle noise components with SSPs.

MEG source mapping. We source imaged the resting-state MEG sensor data using the coregistered anatomy folder provided by HCP(*28*). We computed MEG biophysical head models for each participant using the *Brainstorm* overlapping-spheres model (default parameters) applied to 15,000 locations distributed over the entire cortex. Source maps for each participants' recording were computed using linearly-constrained minimum-variance (LCMV) beamforming (using *Brainstorm*'s default parameters: 2018 version). Noise statistics were estimated from the empty-room recordings collected on the respective day of visit of each participant. Individual source maps were then projected onto a default anatomy template, spatially smoothed (3mm) and clustered into the 200 cortical regions of the Schaefer atlas(*83*) using the first principal component within each region as representative time series of brain activity. Brain-fingerprints were derived from the power spectrum densities (PSD) of these regional source timeseries computed using Welch's method with a sliding window of 2 seconds and 50% overlap.

Correspondence of salient neurophysiological traits and heritable brain phenotypes. We determined whether the salient features for individual differentiation were aligned topographically with heritable brain phenotypes. To do this, we computed the Pearson's spatial correlation of ICC neurophysiological profile topographies with the brain maps obtained from the heritability analyses (see **Heritability of brain phenotypes**) across the 200 regions of the Schaefer atlas(*83*). We controlled for the spatial autocorrelation of the data using the Hungarian method (*91*, *92*) (see **Correction for spatial autocorrelation of brain maps**).

Neuroanatomy. We verified that the neurophysiological profiles of MZ twin pairs matched in spite of heritable neuroanatomical features. We, therefore, derived structural statistics for each region of the Desikan-Killiany atlas from *Freesurfer*(*93*). We then i) computed the heritability of these features following the procedure described in the main text, and ii) tested for a possible linear association between anatomical and spectral similarity across twin pairs. The results are reported separately for MZ, and DZ twin pairs (see The Matching Between the Neurophysiological Profiles of Monozygotic Twins Is Not Driven by Anatomy).

Biophysical and environmental artifacts. We investigated whether MEG recording artifacts might have overly contributed to the differentiation between individuals. We computed the root-mean-squares (RMS) of ocular and cardiac reference signals (ECG, HEOG, VEOG, respectively) collected simultaneously with MEG data. We then linearly regressed these measures from the neurophysiological profiles and used the residuals of this regression to differentiate individuals.
We then tested whether the environmental and instrument noise conditions on the day of the MEG recordings biased individual differentiation(*2*). We, therefore, used the empty-room recordings collected on the same day of the MEG session for each participant to derive pseudo neurophysiological profiles. These empty-room recordings were preprocessed using the same filters as the resting-state data and projected onto the participant's brain using the same imaging kernels. We computed the differentiation accuracies obtained based on these pseudo-profiles.

Gene expression data. Gene expression data were obtained from the six postmortem brains provided by the AHBA (http://human.brain-map.org/)(*33*) using the *abagen* Python package(*35*), following a pipeline published previously(*32*). In brief, we first used microarray probes with the highest differential stability to represent gene expression for each gene (20,232 in total). Tissue samples were assigned to each of the 200 brain regions of the Schaefer atlas using Montreal Neurological Institute (MNI) coordinates generated via nonlinear registrations. We ignored tissue samples further than 2 mm away from each brain region. To reduce potential misassignment, sample-to-region matching was constrained by hemisphere and to the cortex. If a region of the Schaefer atlas was not assigned a sample, the closest sample in Euclidian distance to the centroid of the region was selected. Gene expression was normalized across tissue samples and subjects, and for each of the retained genes, was obtained by averaging across donors. We retained 9104 genes with a differential stability above 0.1 in further analyses, following good-practice guidelines and previous literature(*32*, *34*, *35*, *84*).

Cross-validation of gene-differentiation PLS analysis. We assessed the robustness of our PLS model through cross-validation of Pearson's correlation between the observed gene scores and ICC statistics. We followed the same cross-validation procedures as Hansen and colleagues(*32*), splitting brain regions into one testing and one training set. A random seed was used to determine the training set: 75% of the brain regions the closest in Euclidian distance to the seed location were used to train the PLS model. The quartile of regions were held out to test the PLS model by computing the correlation between predicted gene scores and ICC statistics [*Corr(XtestUtrain, YtestVtrain*)]. This procedure was repeated 100 times to produce a distribution of correlations. The significance of the cross-validation outcomes was assessed against a null model obtained from spatial autocorrelation-preserving permutations of the gene expression matrix and repeated the cross-validation procedure 1,000 times (Figure S5c).

Gene expression & psychological-processes PLS analysis. We assessed the relationship between gene expression and psychological processes as indexed by brain activation maps obtained from *Neurosynth*(*80*).

The brain map associated with each psychological-process term represents the probabilistic association between this term (e.g., attention) and brain activations observed at each voxel from

published studies reporting on that psychological process. This meta-analytic approach combines data from >14,000 published fMRI studies. We focused our analyses on the 123 terms reported by Hansen and colleagues(*32*) at the intersection between Neurosynth(*80*) and the Cognitive Atlas(*94*), a public ontology of cognitive science. This data-driven approach did not distinguish between activations and deactivations, nor did it consider the degree of activation of a given brain area. Here too, we used the Schaefer-200 atlas(*83*) to sample the resulting cortical maps.

We assessed the alignment between the respective latent components associated with gene-psychological processes and gene-differentiation by computing the Pearson's correlation between gene scores and PLS loadings (Figure S6).

Gene ontology analysis. To determine the biological processes contributing to positively and negatively loaded genes, we performed an enrichment analysis for the 50% largest loadings (e.g., genes with the 50% most negative and positive loadings) using the ShinyGO V 0.77 (Dec 20th 2023) gene ontology tool(*36*) and the GO pathway databases of biological processes(*89*). Genes with no Entrez Ids were ignored. Fold enrichment for each biological process was computed by comparing the frequency of a given biological process in the set of positive genes to the frequency of that process in the entire genome. P-values associated with fold enrichment for all terms were corrected for false discovery rate (FDR). See Supplemental Data for a comprehensive list of all biological processes and their corresponding fold enrichment values.

Development of the gene signature. We binned gene expression data from BrainSpan(*49*) into five life stages: fetal (8–37 post-conception weeks), infant (4 months–1 year), child (2–8 years), adolescent (11–19 years) and adult (21–40 years)(*95*). For each life stage, we computed the gene expression of the top 50% of positively and negatively loaded genes for each cortical region. Additionally, we computed gene expression at every neurodevelopmental stage for a random set of genes (Figure S7B). Note that of the 16 cortical regions with gene expression data, four regions only had samples for the fetal stage; therefore, we report data for the 12 cortical regions with data across all neurodevelopmental stages.

Human accelerated region analyses. We defined genes associated with human accelerated regions (HARs) based on previous work by Wei et al.(*96*). Of the 1711 genes featured in AHBA, they reported that 415 genes were significantly more expressed in brain tissues than other available body samples (see Supplementary Data 2 therein). We used these 415 HAR-brain genes for further analyses, including 313 genes that were differential stable in our analysis (see **Gene expression data**). We first assessed the overrepresentation of HAR-brain genes in the identified gene signature (top 50% positive and negative loadings) through permutation analyses. We then assessed the spatial correspondence of gene expression of HAR-brain genes and the computed gene brain score (see **Correction for spatial autocorrelation of brain maps**).

Supplementary Results

Assessing the Robustness of Neurophysiological Profiles

We performed a series of sensitivity analyses to rule out the possibility of environmental and physiological artifacts affecting our results.

We first evaluated the influence of environmental factors that may affected the MEG recordings. We processed empty-room recordings in the same way as the actual participant data to derive pseudo neurophysiological profiles related to the environmental conditions around each participant's visit. Individual differentiation was poor based on these pseudo neurophysiological profiles (<1.7%; Figures 1B).

We then used linear regression models to remove the variance associated with physiological artifacts from the neurophysiological profiles (see Methods (Cont'd.) **Biophysical and environmental artifacts**). Using the same analysis pipeline, we observed that identification accuracy remained largely unaffected: 82.6% [74.7, 89.3] differentiation accuracy across all participants, 55.2% [46.7, 66.7] matching accuracy between monozygotic twins, and 5.8% [0.0, 15.0] between dizygotic twins, using broadband features (Figure S1). The robustness of the results indicates that individual differentiation is not significantly driven by physiological artefacts.

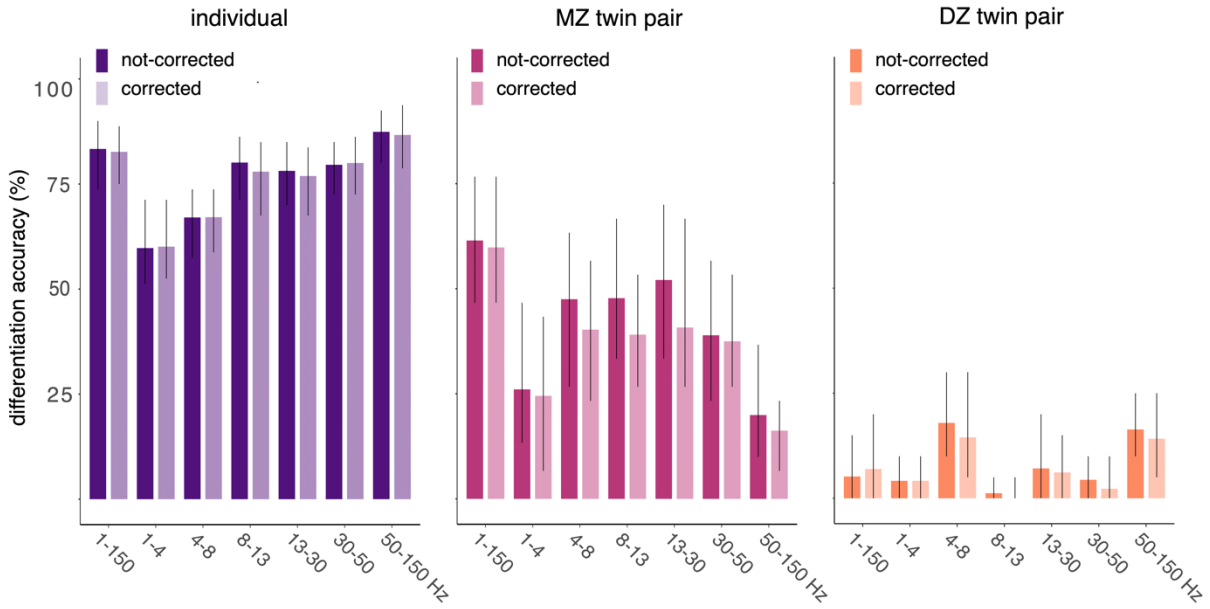

Fig. S1. Physiological artifacts do not impact differentiation accuracy.
Comparison of the differentiation and twin-matching accuracy scores before and after regressing out the influence of artifacts on neurophysiological profiles, for singletons (left panel), MZ twin pairs (middle panel) and DZ twin pairs (right panel).

The Matching Between the Neurophysiological Profiles of Monozygotic Twins Is Not Driven by Anatomy

We tested whether the matching between the neurophysiological profiles of MZ twins may have been driven by similarities in their brain anatomy. The brain structural features of MZ siblings extracted from *Freesurfer*(*93*) were indeed more similar than those of DZ twins or unrelated participants (see Methods): they showed high correlation between MZ siblings (r= 0.99), and lower for DZ twin pairs (r= 0.93). The most heritable brain anatomical features the most heritable were related to the curvature (h= 1.75) and thickness (h= 1.75) of the cortex.

To assess the extent to which these brain structural features contributed to the heritability of neurophysiological profiles, we estimated the linear correlation between the matching of neurophysiological profiles of twin siblings and the similarity of their respective brain anatomical features (Figure S2A and Methods). These relationships were not statistically significant between MZ siblings (r= 0.32, p= 0.06) not between DZ siblings (r= -0.22, p= 0.32; see Figure S2B right panel). The outcome was similar when we replicated this analysis for neurophysiological profiles derived from alpha-band (MZ: r= 0.31, p= 0.08; DZ: r= -0.17, p= 0.45) and beta-band (MZ: r= 0.32, p= 0.07; DZ: r= -0.15, p= 0.51) brain activity. Bayes factor analyses corroborated that there was little evidence for a relationship between similarities of structural and neurophysiological traits (Supplemental Table S1). To conclude, while brain curvature and cortical thickness are heritable brain phenotypes, they did not contribute significantly to individual differentiation based on their neurophysiological profiles.

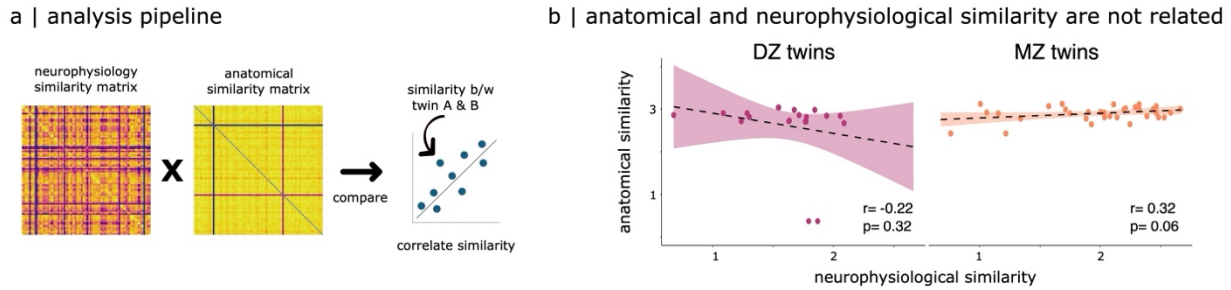

Fig. S2. Twin Matching is Not Driven by Brain Anatomical Similarity.

(a) Analysis pipeline to test for a possible linear association between brain anatomical and neurophysiological traits. The anatomical and neurophysiological features across MZ and DZ twin pairs were Fisher-transformed and their association tested for linear relationship. (b) Scatter plots and best linear model of the association between brain anatomical neurophysiological traits across MZ and DZ twin pairs.

	Pearson's r		BF_{10}	
	MZ	DZ	MZ	DZ
Anatomy vs. broadband neurophysiology	0.32	-0.22	1.65	0.68
Anatomy vs. alpha-band neurophysiology	0.31	-0.17	1.46	0.57
Anatomy vs. Beta-band neurophysiology	0.31	-0.15	1.60	0.54

Table S1: Pearson's Correlations Between the Similarity of Brain Anatomy and Neurophysiological Profiles.

We fit linear models relating the similarity of brain anatomical similarity and neurophysiological profiles derived from broadband, alpha band, and beta band activity between MZ and DZ twin siblings. There was little Bayes factor evidence (BF_{10}) of such a relationship.

Salient Features for Participant Differentiation are Heritable

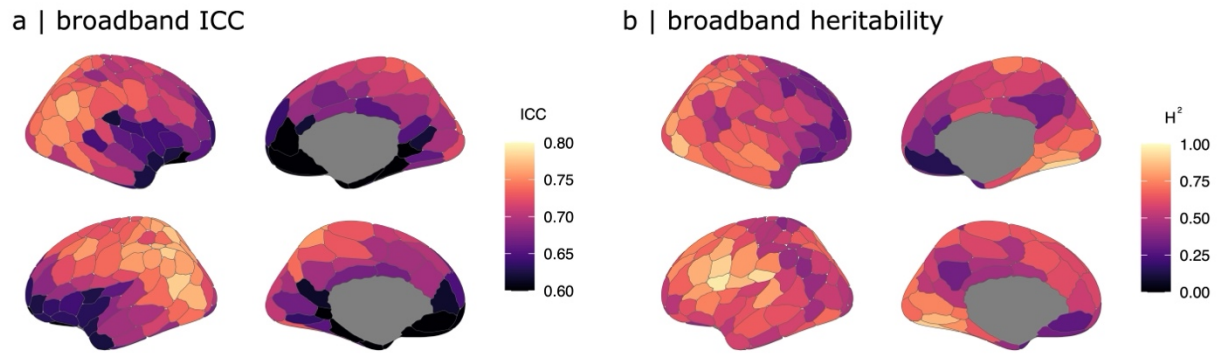

Fig. S3. Salient regions (measured with ICC) of the broadband neurophysiological profile and its heritable brain phenotypes.

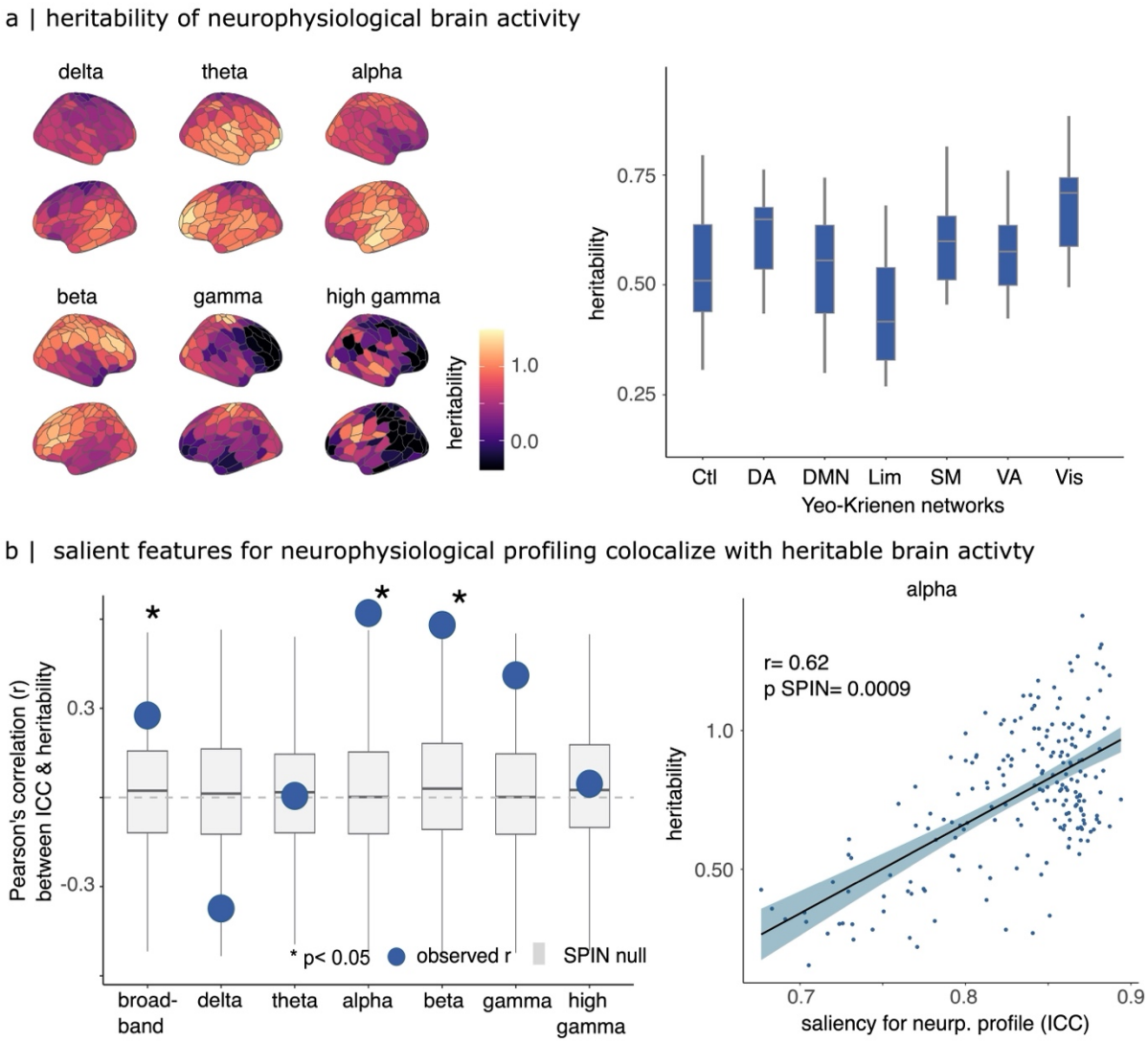

Figure S4: Differentiable Neurophysiological Traits are Heritable.

(a) Left panel: Cortical maps of heritability of neurophysiological traits derived from Falconer's equation. High heritability values highlight the regions which neurophysiological activity is most influenced by genetics.

Right panel: Heritability scores of broadband neurophysiological traits are reported per region of the 7 Yeo-Krienen atlas of resting-state networks, highlighting variations in heritability across brain systems.

(b) Left panel: Pearson's correlation between the neurophysiological traits that are the most salient for individual differentiation and their heritability, for each tested frequency band of electrophysiology. The blue dots indicate the correlation statistics and the boxplots depict the null distributions obtained by spin-test permutations.

Right panel: Scatter plot of best linear model relating the heritability and saliency of alpha-band neurophysiological traits. Each dot represents a region of the Schaefer-200 atlas. The saliency of the alpha-band neurophysiological traits for individual differentiation is linearly related to their heritability. This further demonstrates the genetic influence on neurophysiological traits.

PLS Analysis Pipeline & Gene-Differentiation Signature

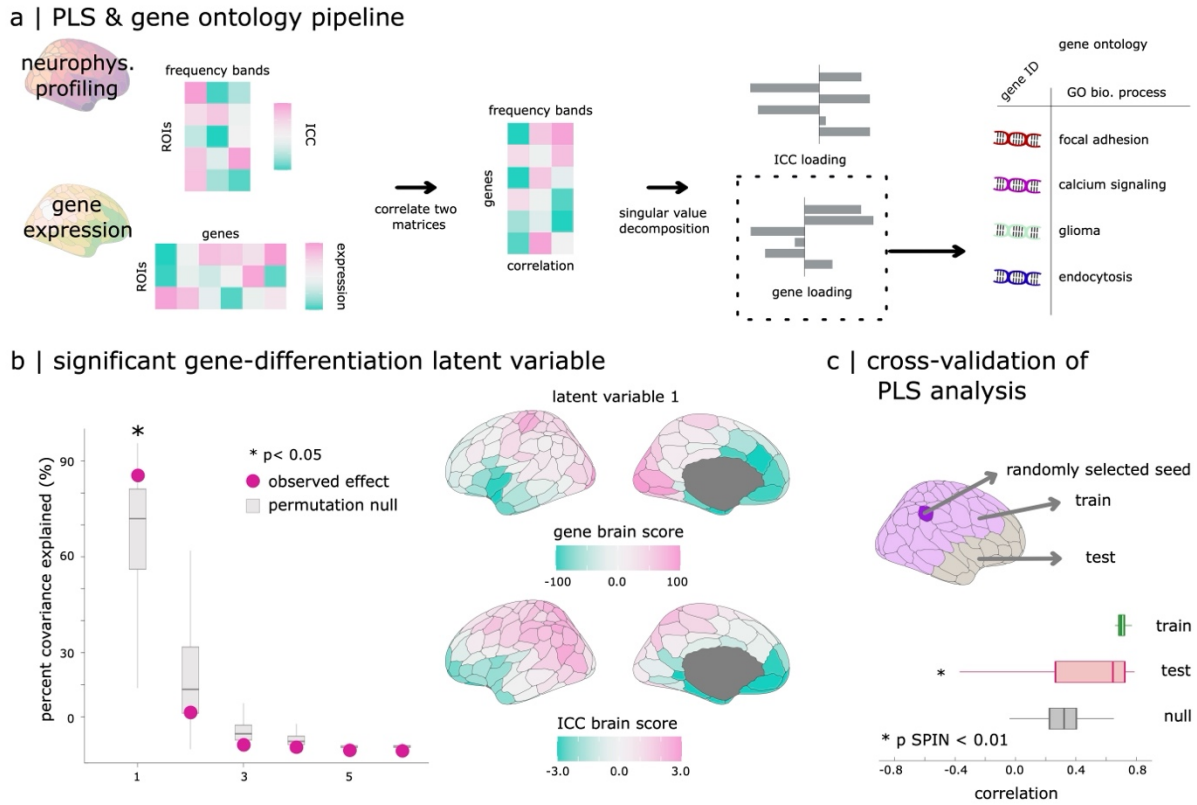

Figure S5: Analysis Pipeline and Outcomes of Gene-Differentiation PLS Analysis.

(a) Analysis Pipeline: Two data matrices were submitted to a Partial-Least-Squares (PLS) and gene ontology analysis: i) the first data matrix gathered the most salient traits for neurophysiological profiling; ii) the second data matrix contained scores of gene expression across the regions of the Schaefer-200 cortical atlas(*83*). The PLS analysis resulted in latent components capturing the modes of largest covariance between these variables. Using the elements with top loadings, we performed a gene ontology analysis to determine if the contributing genes were enriched for specific molecular processes.

(b) Cortical Topographies of Latent Components: The left panel shows the PLS latent components with pink dots, ordered by decreasing effect size. Statistical significance was determined with 1,000 permutations of the observed data, with spatial autocorrelation correction applied, highlighting only the first latent component. The right panel shows the related cortical topographies of gene-expression and ICC scores derived by projecting this first latent component onto the observed data.

(c) Cross-validation Process of the Gene-Differentiability PLS Analysis: We trained the PLS model using 75% of the cortical regions, selected based on their proximity in Euclidean distance to a randomly selected seed (dark purple regions), and tested the relationship between gene-expression and ICC scores on the rest of the data. The median out-of-sample relationship observed was r= 0.64 (p_{spin}= 0.002).

Psychological Processes and Differentiation

We assessed the similarity in gene-expression brain score between the outcomes of the gene-differentiation and gene-psychological processes PLS analyses. We found strong linear relationships between the identified gene scores and the PLS loadings (Figure S6 and The Gene-Differentiation Gradient Correlates with Psychological Processes).

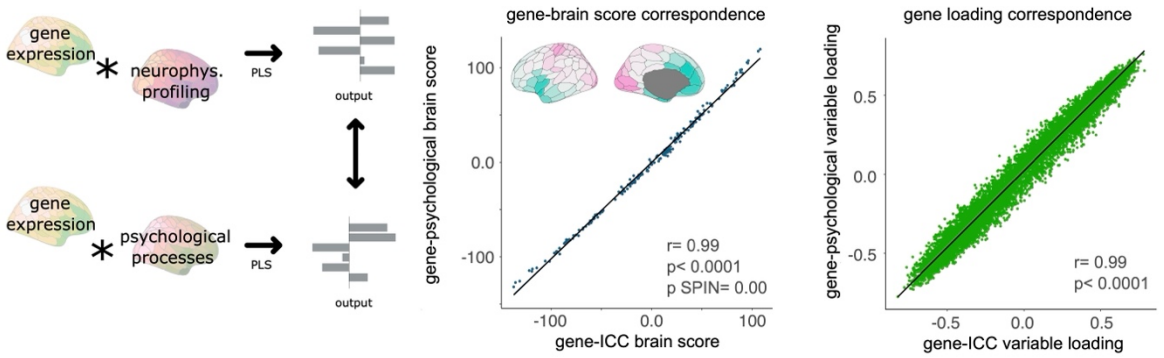

Figure S6: Covariance of Gene Latent Component with Psychological Processes and Neurophysiological Differentiation.

The middle panel features a scatter plot of gene-expression scores from both the outcomes of the gene-differentiation and gene-psychological processes PLS analyses. We found a strong linear relationship indicative of similar patterns in gene expression relating both neurophysiological differentiation and psychological functioning.

The right panel shows a scatter plot of gene loadings for both PLS analyses, again indicating a high degree of correspondence, with genes contributing to differentiation also relevant to psychological processes. The correlation coefficients and p-values indicated report the statistical significance of these relationships.

We further tested whether the outcome of the PLS analysis for psychological processes (see Main Text) covaried with individual differentiation. We anticipated such a relationship as both psychological processes and individual differentiation covary with similar gene expression signatures. The PLS of psychological-process and individual differentiation featured a single significant latent variable (p= 0.002) that explained 87.0% of the covariance between these variables (85.2% covariance explained, p_{SPIN}= 0.002, 95% CI = [54.24., 87.37]). The ICC loadings and psychological process term loadings were linearly related to the loadings obtained from the previously reported PLS analysis (ICC loadings similarity, r=0.78; term loading similarity, r= 0.92).

The Gene-Differentiation Signature Overexpresses Genes Involved in Human Evolution

To assess the evolutionary significance of the gene-differentiation signature, we examined its association with human-accelerated regions (HARs) of the genome. HARs are critical loci linked to the evolutionary expansion of cortical areas involved in higher-order cognition(*96–99*). We found an overrepresentation of HAR-Brain genes in the gene-differentiation signature (p = 0.004; Supplemental Data 2). Further, there was a significant topographical alignment (negative spatial

correlation) between the cortical distribution of these HAR-Brain genes and the gene-differentiation signature (r= -0.63, p_{spin}= 0.001; Figure S7A).

This finding highlights the evolutionary and developmental significance of these genomic regions. HARs, the most rapidly evolving segments of the human genome, are crucial in neurodevelopment(*98*) and modulate susceptibility to psychiatric neurodevelopmental disorders(*97*, *100*). Additionally, HAR gene expression is linked to cortical expansion and predominantly occurs in regions involved in higher-order cognitive processes(*96*, *101*).

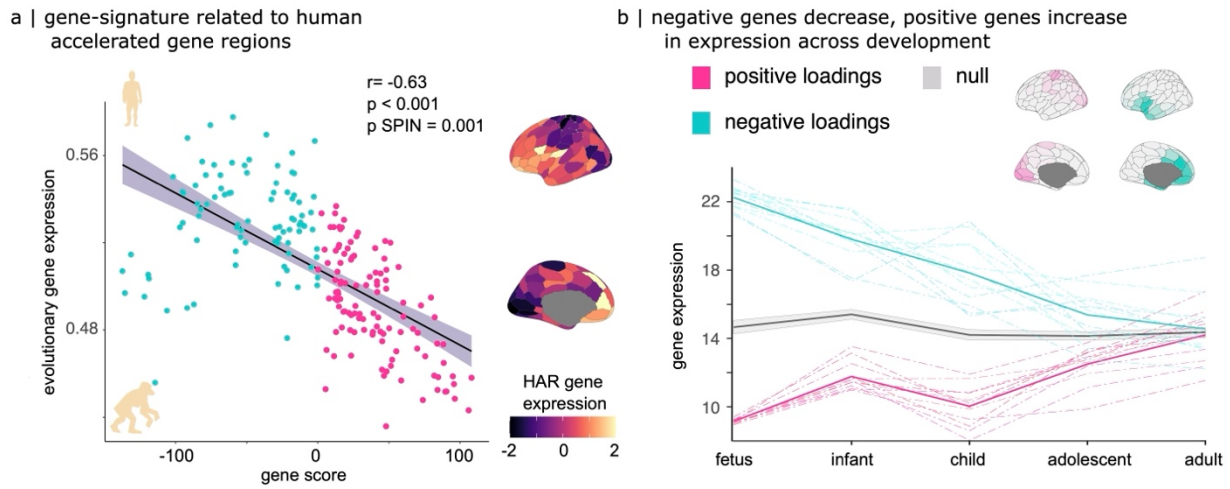

Figure S7: Relationship Between Gene Signature, Human Evolutionary Expansion, and Neurodevelopmental Maturation

(a) Evolutionary Genomics and Gene Score Correlation: The left panel displays a scatter plot contrasting gene scores from the PLS analysis against the expression of HAR-brain genes, which are implicated in the evolutionary expansion of the human brain. Dots are color-coded, with pink (blue) indicating regions of positive (negative) gene scores. There is a linear negative relationship between these gene scores and the expression of HAR genes. The right panel shows z-scored maps of the cortical distribution of HAR gene expression.

(b) Developmental Trajectory of Gene Expression: The line plot displays the gene expression of the top-50% negatively (blue) and positively (pink) loaded genes across five developmental stages (fetal, infant, child, adolescent, and adult). Dotted lines represent the cortical regions shown in the top right corner, with their respective averages shown with solid lines. The grey line shows the mean expression trajectory of randomly selected gene sets.